Adaptive Assist Control Based on Impedance Model of Pneumatic Gel Muscle and Its Application in Augmented Walking Suit

(空気圧ゲル人工筋のインピーダンスモデルに基づく
適応支援制御と拡張歩行スーツにおけるその応用)

by

THAKUR CHETAN PRAKASH

Graduate School of Engineering
Hiroshima University
March, 2020

Contents

List of Figures

List of Tables

Chapter 1

Introduction

1.1 Background and Motivation

The ability to move without interruption is one of the critical functions of the human body. It is one of the reasons for enjoying a good quality of life by performing a variety of daily tasks independently. However, there are many instances, such as aging, accidents, and longer and stressful working conditions that result in muscle fatigue and injuries, making it difficult to walk, thereby affecting the quality of life of the individual. Such situations can be avoided or addressed using exoskeletons or wearable assistive devices. The muscle activation pattern of human gait is dynamic, and it changes as the motion or intent is changed, but the basic pattern of the gait cycle is remains same. While developing the AWS, we considered such factors as the nature of the work area, age, flexibility for use it outdoors, light weight, portability, ease of use, reduced muscle effort during walking, and no impact on the normal gait cycle. With an increasing elderly population, stressful work condition devices like this will play a significant role in improving the quality of life. Garon et al. [1] mentioned that there is demand for assistive devices for mobility for people such as the elderly, the disabled, and healthcare staff for various tasks involved in daily life. Among various lower-limb assistive devices, there is a tradeoff between autonomous actuation, wearability, light

weight, and affordability. HAL [2] makes walking easier for the elderly and supports rehabilitation for post stroke or accidents. Wearable agri robot [3] was designed for supporting farming activities and reduce muscle fatigue, it supports body posture and reduces the muscle fatigue. An walking assist device was designed for walking with a body weight support system [4] for augmenting walking and assisting the squatting motion required for pick-and-place tasks in various work environments. The RoboKnee [5] is one degree of freedom (DOF) exoskeleton designed to support human locomotion, such as walking and stair climbing. A plantarflexion assist exoskeleton [6] is designed to reduce the metabolic cost of walking.

A tethered bilateral hip extension and plantarflexion exosuit [7] was tested for assistance magnitude and changes in the metabolic cost of walking, and a reduction in metabolic energy by 22.8% while walking. A soft exosuit for hip assistance provides 30% of the biological torque moment for gait [8] by using a spooled-webbing actuator connected to the back of the thigh. The Myosuit, an untethered biarticular exosuit, reduces EMG activities during the sit to stand transfer motion by 26% [9]. Unilateral exosuit support for ankle plantarflexion and dorsiflexion were reported to reduce the metabolic rate of gait by 16% [10]. A soft inflatable exosuit for knee rehabilitation [11] reduces muscle activity in the rectus femoris by 7%. A biologically inspired soft exosuit for walking assistance [12] showed an average metabolic reduction of 5.1% during walking. A passive unpowered exoskeleton reduces metabolic cost of gait by 7% [13].

These devices are divided into segments, such as healthcare, disability support, and augmenting locomotion. These devices augment human motion significantly based on the reduction in EMG activities and metabolic rate during walking, but their use in outside environments is limited, especially in agriculture and factory settings. For

augmented walking, wearability, light weight, portability, ease of use and reduced muscle fatigue, are essential but together missing in the assistive devices discussed above. To solve this problem, we previously developed a lightweight, low-powered pneumatic gel muscle (PGM) [14] as shown in Fig 2.3. The PGM can generate force with 60 kPa air pressure, which is not possible with the McKibben pneumatic artificial muscle (PAM) [15]. It is also structured to be stitched to fabric or fix using Velcro tapes; this makes it easy to design the assistive suit.

In [14], we devised the concept of an unplugged powered puit (UPS) for walking assistance using the advantage of the PGM and the gait cycle. The UPS is a passive walking assist suit in which the air pressure required for actuating the PGM is generated by placing a rubber pump at the heel of the shoe. This configuration enables a limb in stance phase to generate the assistive air pressure required for the contralateral limb in the swing phase. The pump in the shoe can generate air pressure up to 50 kPa. The challenges of this configuration, as discussed in [14], are actuation delay due to the long distance between pump and PGM; the UPS cannot be used for a walking pitch of faster than two steps per second. Another limitation of the UPS is the use of the pump in the shoe. To support multiple muscle groups, more pumps are needed in the shoe, which is not suitable for use in an outside environment because of possible leaks in the pump and the difficulty of walking with pumps in the shoe. In [14] evaluation of the UPS was done based on only four muscles of the lower limb, and only the rectus femoris showed a reduction in muscle activity by 20% whereas others showed no change. To overcome these challenges of the UPS, we developed the AWS in which an air tank replaces the pumps and actuation control is designed using force sensitive resistor (FSR) sensors in the shoe. This change solves the problem of supporting variable walking speeds, providing the ability to support multiple muscle groups using additional PGM.

1.2 Content Outline

The thesis is organized as follows:

In chapter 2, we discuss the design and development of an augmented walking suit. Augmenting or assisting human motion requires understanding of motion and motion planning. A detailed gait cycle classification and contralateral foot orientation-based model is explained to identify individual gait phases. We used pneumatic Gel Muscle for actuator in AWS. We developed impedance model of PGM by experimenting and measuring impedance characteristics. Based on these, we assist control strategies are developed and implemented using gait phase detection algorithm.

In chapter 3, we discuss the evaluation methods of the augmented walking suit. The effectiveness of AWS was studied using biomechanical simulation. Changes in muscle force and kinematics during one gait cycle are measured and evaluated. A customized simulation of PGM model is developed for this study. Physiological evaluation experiment was conducted where subjects wore the AWS and conducted walking experiments with different assistive force and control algorithms. Subjects were selected randomly and could rest or stop the experiment if they wish to. The effect of AWS on muscle activation was studied by conducting statistical analysis on normalized average sEMG data.

In chapter 4, we discuss the plot trials conducted to study the adoption of AWS in rural areas for elderly and small and independent farmers or workers. This project was conducted in collaboration with PhD students in other graduate schools at Hiroshima University. We studied how social and cultural aspects affect adoption of wearable assist suits. The pilot trial was focused on elderly and independent farmers.

In chapter 5, we discuss the summary of the study and future scope.

Chapter 2

Development of Augmented Walking Suit

2.1 Introduction

As discussed earlier, out of many method of developing walking assistive and augmentation devices we aimed to developed lightweight wearable design. To developed such device we needed actuators that can placed and fixed using soft materials completely eliminating the need of hard structures. We also need a strategy to detect the walking motion if classification of gait phases and actuation control support the design paradigm of our object. In this capter we we will discuss the human gait and classification in details from special and kinematics point of view, assistive region of gait cycle and its requirements and modeling gait cycle timing for different phase of our interest.

2.2 Human Gait Cycle

Jacqelin perry, 2010 gait cycle is very complex and varies from person to person and depends on the gait deformity due to diseases such as cerebral parsley, paralysis or polio. These situation makes it difficult to design and implement the assistive or artificial limb due to gait deviation. Therefore, perry et al. developed generic terminology for

functional phases of the gait cycle which directly identifies gait phase and motions at various joints of the limb. The phases of gait provide mean for correlating the simultaneous actions of the individual joints into pattern of total limb function. This is important to interpret the functional effects of disability, the relative difference in joint motion compared to other and a posture which is suitable in on gait phase is not suitable for next as the functional needs to maintain body posture changes. As a result, the both timing and joint angles are very important which increase the complexity of the gait cycle. Understanding this phases and the pattern not only help in gait analysis bu there are many researchers who have used these patterns as a signature to provide assistance and derived methods for rehabilitation. In our study, we used it as a method for providing assistance to assist forward locomotion of the gait cycle.

2.2.1 Classification of Gait Cycle

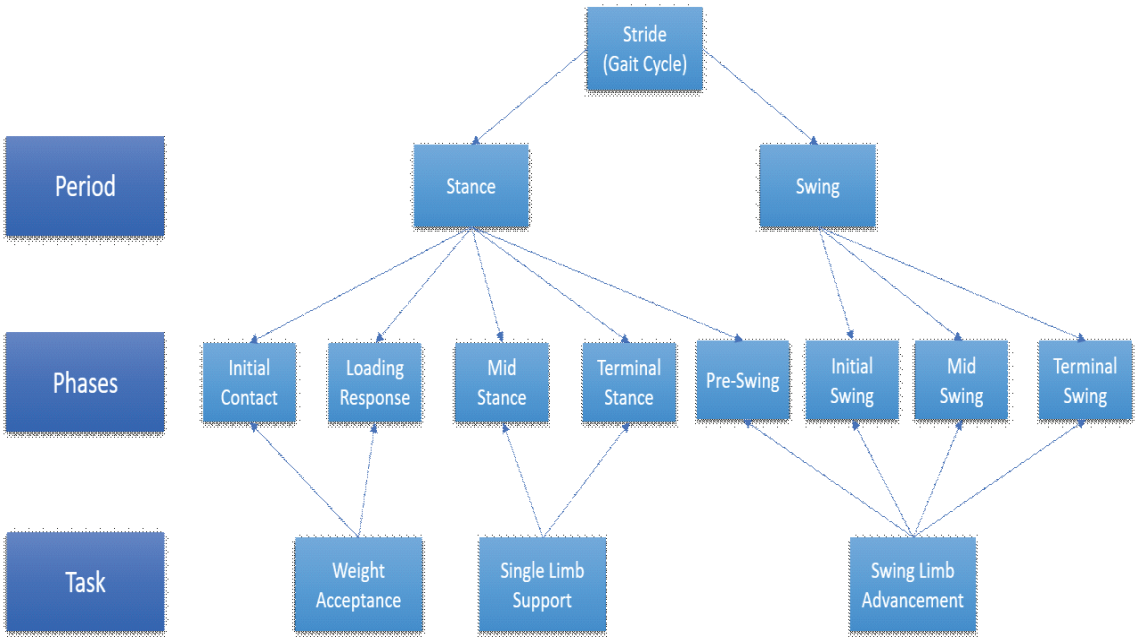

Fig. 2.1: Gait Cycle, phases of gait cycle and division of phases into tasks

The human gait cycle which is also called stride which is cyclic motion of lower limd performed during walking or running. In our study we focused on walking. The stride is primarily divided into two major phase which is also period of the lower limb either on the ground or in the air, these are called stance and swing phase respectively. Figure 2.1 describes the gait cycle two major phase in gait cycle and their respective sub phases classifications and physical task conducted in these phases. These sequential combinations of the phases of the gait enabled the limb to accomplish 3 tasks i.e. weight acceptance (WA), single limb support (SLS), and single limb advancement (SLA).

Figure 2.2 describes gait cycle in terms of limb and foot orientation and their respective phases in the gait cycle for one limb.

WA is the first task of the gait cycle and the most challenging because it addresses the three demands of the gait which are shock absorption, initial limb stability and the preservation of progression. The challenge is abrupt transfer of body weight onto the limb which has just finished the swinging forward and has unstable alignment. To answer the challenge this task involves two phases initial contact (IC) and loading response (LR).

Initial contact includes the instant the foot is drops on the floor and immediate reaction to the onset of body weight transfer this phase lasts for 0 to 2% of GC. This is followed by loading response (LR), it exists in the interval of 2 to 12% of gat cycle and contained in the initial double stance period. The phase is part of double limb support with the objectives of shock absorption, weight bearing stability and preservation of progression.

SLS constitutes of two phases mid stance (MS) and terminal stance (TS). MS convers 12% to 31% of the GC, this is the first half of the SLS, it begins with the lift of the other limb and continues as the body weight is aligned over the forefoot. TS

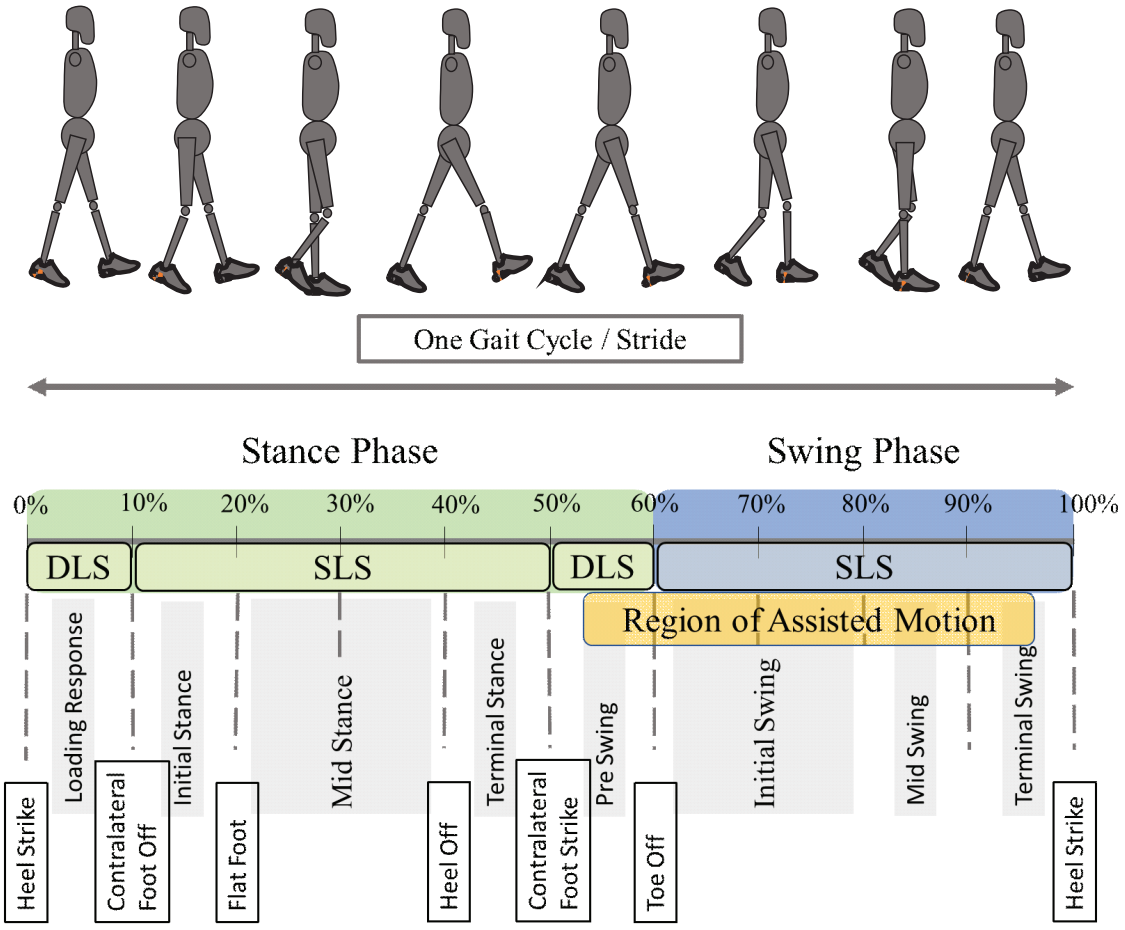

Fig. 2.2: Detailed gait classification with foot orientation and region of assistance defined for Augmented Walking Suit.

complete SLS and consists of 31% to 50% of the GC, it begins with the hip rise and continue until the other foot strikes the ground. The body weight moves ahead of the forefoot with the objective of the progression of the body ahead of the supporting limb and stability of limb and trunk.

SLA constitutes of 4 phases pre-swing (PS), Initial swing (IS), Mid swing (MS) and Terminal swing (TS). The objective of this task is to meet the high demands of advancing the limb which begin in the stance phase. PS exists in the interval of 50% to 62% of the GC, the objective of this phase is to prepare position of the limb for swing

phase and accelerate the progression of the limb. This is also final phase of stance which begins with IC of another limb and ends with ipsilateral toe off. As the limb take off the weight transfers to the other limb and muscles are unloaded, the trailing extremity further contribute to the progression with forward push and prepares the limb for the rapid demands of swing. IS consists of 62% to 75% of the gait cycle, the objective of this phase is to have foot clearance of the floor and advancement of the limb from its trailing position. This phase begins with foot lifting from the floor and end when the swinging foot is opposite to the stance foot. MS consists of 75% to 87% of the GC, the object of this phase are limb advancement and foot clearance of the floor. This phase ends when the swinging limb is forward and the tibia is vertical (i.e. hip and knee flexion postures are equal). TS is the final phase and consists of 87% to 100% of the GC, the objective of this phase is to complete the limb advancement and prepare the limb for the stance. This phase finishes the stride of the concerned limb.

WA, SLS and SLA all perform important tasks to maintain body posture and moving forward. SLA is responsible for taking to limb forward in gait cycle. This task takes requires effort to lift and move the limb forward with hip flexsion and knee extension as well as taking the load while terminating the swing phase.

2.2.2 Modeling Gait Cycle

We discussed the synchronous gait cycle and spatial and temporal characteristics in the previous section. In this section, we will define the gait model in terms of time of each major phase of the gait cycle i.e. stance and swing phase of the gait cycle using information from both the limbs.

Our objective is to identify the swing time for each limb while walking. For our purpose we defined simple generic model which will provide time of stance ans swing phase of the gait cycle. We defined following terms for our model.

$$SWT = Swing\ Time\ of\ lower\ limb$$

$$SPT = Stance\ Time\ of\ lower\ limb$$

$$DST = Double\ Limb\ Support\ Time\ of\ lower\ limb$$

$$SST = Single\ Limb\ Support\ Time\ of\ lower\ limb$$

SWT duration of time when limb is in the swing phase, SPT duration of time when limb is in the stance phase. DST is the duration of time for double limb support i.e. when both the limbs are on the ground. SST is the duration of time where single limb supports body weight while other limb is in swing phase going forward.

The duration of each defined above are identified by the changes in the motion by using sensors e.g. inertial measurement units (IMU), force sensors. To correctly find the swing time of the limb while walking we defined general framework for detecting duration and time of respective of gait phases for each limb.

From the gait classification we knew that the swing phase is the time between toe off to heel strike of the limb while the contralateral limb is in the stance phase i.e. single limb support SST. We defined this relations in following equation where SWT is difference in time of toe off and heel strike and SST is same is SWT

$$SWT = T_{ToeOff} - T_{HeelStrike}$$

$$\mathrm{SST}_L = \mathrm{SWT}_R$$

$$\mathrm{SST}_R = \mathrm{SWT}_L$$

The duration of stance phase is difference in timing of heel strike and toe off. Earlier we learnt that the double limb support phase is the duration in gait cycle where both limbs are on ground and makes the transition from one major phase to

another. Therefore difference in stance and swing time duration will be the time where double lime support happens.

$$SPT = T_{HeelStrike} - T_{ToeOff}$$

$$DST = \mathrm{SPT}_L - \mathrm{SWT}_R$$

$$DST = \mathrm{SPT}_R - \mathrm{SWT}_L$$

The above equation explain when left and right limb in swing i.e. SWT_R and SWT_L we get duration of double limb support.

2.3 Pneumatic Gel Muscle

2.3.1 Overview and Design

A PAM is a lightweight flexible actuator driven by pneumatic pressure. The McKibben artificial muscle is the most popular PAM. Its behavior is similar to that of biological muscles. The McKibben artificial muscle comprises an inner tube surrounded by braided mesh. The inner tube is made of a stretchable rubber tube and the braided mesh provides protection and controls contraction of the artificial muscle. The pantograph structure of the braided mesh allows the muscle to extend and contract easily. The contraction of the actuator depends on the air pressure and volume and the non-extensibility of the braided mesh shortens and produces tension if the endpoint is attached to a load. Such actuators are favorable for motion assist because of their similarity to human muscle functions. The conventional McKibben actuator requires high pneumatic pressure and volume depending on the size of the muscle. Therefore, even when the McKibben actuator is light and flexible, it is not suitable for soft and wearable motion-assist devices owing to the requirement of a compressor or an air tank and a controller of the air pressure and volume flow for driving the pneumatic actuator.

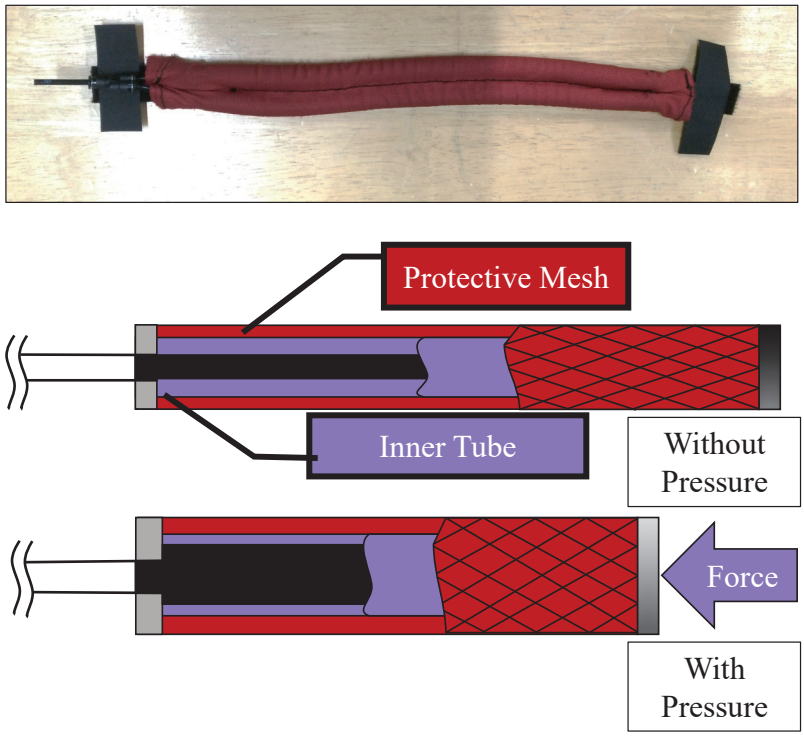

Fig. 2.3: Pneumatic gel muscle and illustration of force generating mechanism.

The present paper proposes improving the material of the inner tube to make artificial muscles that are driven under very low air pressure and volume.

Figure 2.3 outlines the structure of the PGM, which is the low-pressure-driven PAM developed in this research. The structural design of the PGM follows a principle similar to that of the conventional McKibben artificial muscle in that the PGM has an inner tube and external braided mesh; however, there are changes in the material and configuration that improve performance under the condition of low air pressure. Traditional work [9,10] revealed that the stiffness or elasticity of the inner tube affects the efficiency, force capacity, and contraction range of the PAM. When using an inelastic inner tube and applying higher air pressure, artificial muscles have greater force carrying capacity and efficiency. This means that the air pressure required for actuating artificial muscles can be reduced using an inner rubber tube that is more elastic or

viscose. Additionally, in the case of the conventional McKibben muscle, the length of the braided mesh is the same as that of the inner tube. This configuration of the muscle prevents stretch in the muscle when no pressure is applied. The conventional McKibben artificial muscle therefore needs high air pressure and large volume for actuation. In our research, we improved this design such that it works under low air pressure and has a contraction capability when no pressure is applied to the artificial muscle. This was done by foaming the inner tube with flexible gel made of styrene-based thermoplastic elastomer to improve the viscosity and flexibility. Thanks to its thick and honeycomb structure, the surface of the inner tube is easy to be stretched in multiple directions. The flexible gel can reduce the volume inside the rubber tube and increase the flexibility. It contributes the smooth contraction and extension of the actuator. Figure 1(a) shows the prototype artificial muscles with the inner tube of 250 mm, the inner diameter of 4 mm, the outer braided mesh of 500 mm, and the outer diameter of 9 mm.

2.3.2 Impedance Measurement Experiment

The modeling and characterization of PGM is important due to its similarity with biological muscles and to understand actuator compliance with desired system under consideration. In our study we are using PGM as actuator to assist human motion. In earlier study of PGM only stiffness i.e. forces and displacement relation was studied. But the change in total force due to velocity and acceleration of displacement was not measured hence its impedance characteristics and not know. Without which we cannot develop adaptive assistive force algorithms required for providing force for change in velocity and displacement relation.

Researchers have formulated various methods to model or characterize PAM such as empirical modeling based on experimental observation [16], dynamic modeling of

two direction motion by identifying stiffness and damping coefficients [17], design of nonlinear elastic transmission [18], static and dynamic characteristics of pneumatic muscles [19], elastic energy account of pneumatic artificial muscle [20] and impedance estimation of pneumatic artificial muscle [21].

To measure these characteristics, we assumed spring damper model which is suitable to study elastics actuators with variable stiffness. Figure 2.4 shows the generic spring damper model we wish to use in our study.

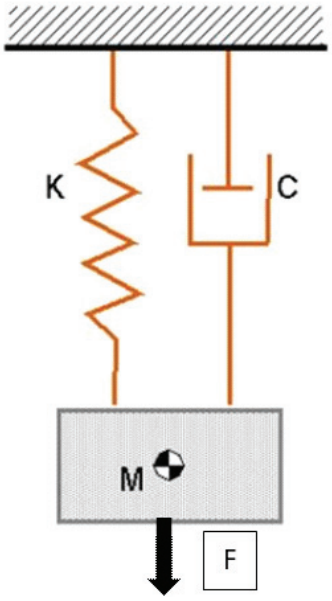

Fig. 2.4: Generic Spring Damper Model used for elastic actuator with variable stiffness and damping characteristics.

Based on the spring damper model the total force generated by the actuators is defined in equation 1 below which includes force components due to stiffness, damping and inertia of the actuator.

$$F(t) = F_m(\ddot{x}(t)) + F_d(P_m, \dot{x}(t)) + F_s(P_m, x(t))$$

Where F_m, F_d and F_s are force due to inertia, damping and stiffness properties of

the PGM.

The variable change in generated force is due to change in the supplied air pressure we modeled the stiffness and damping coefficient. The force stiffness coefficient is sum of natural stiffness and the factor due to change in air pressure. This simplified assumption is derived in below equation.

$$F_s = f\left(x,\ P_m\right) = \ \left(A_{01} + A_{11}P_m\right)\ x;$$

The damping coefficient also follows assumption on similar lines of sum of natural damping coefficient and the factor due to change in air pressure. This simplified assumption is derived in below equation.

$$F_d = f\left(\dot{x},\ P_m\right) = \ \left(D_{01} + D_{11}P_m\right)\ \dot{x};$$

The inertial force is measured as acceleration in displacement and the mass of the actuator as mentioned in following equation.

$$F_m = f\left(\ddot{x}(t)\right) = \ m\ddot{x};$$

Since the mass of actuator i.e. PGM was measured to be very low i.e. 0.025 kg we decided to neglect the force component due to inertia.

x, $\dot{x}$ and $\ddot{x}$ in the above equations are displacement (elongation/contraction), velocity and acceleration of PGM.

To realize the parameters of the model we need to measure force at static displacement as well as dynamic contraction and elongation at various frequencies i.e. velocities.

To measure these, we develop apparatus i.e. experiment setup show in Figure 2.5. The setup consists of a linear slider consisting of lead screw with 5 mm lead

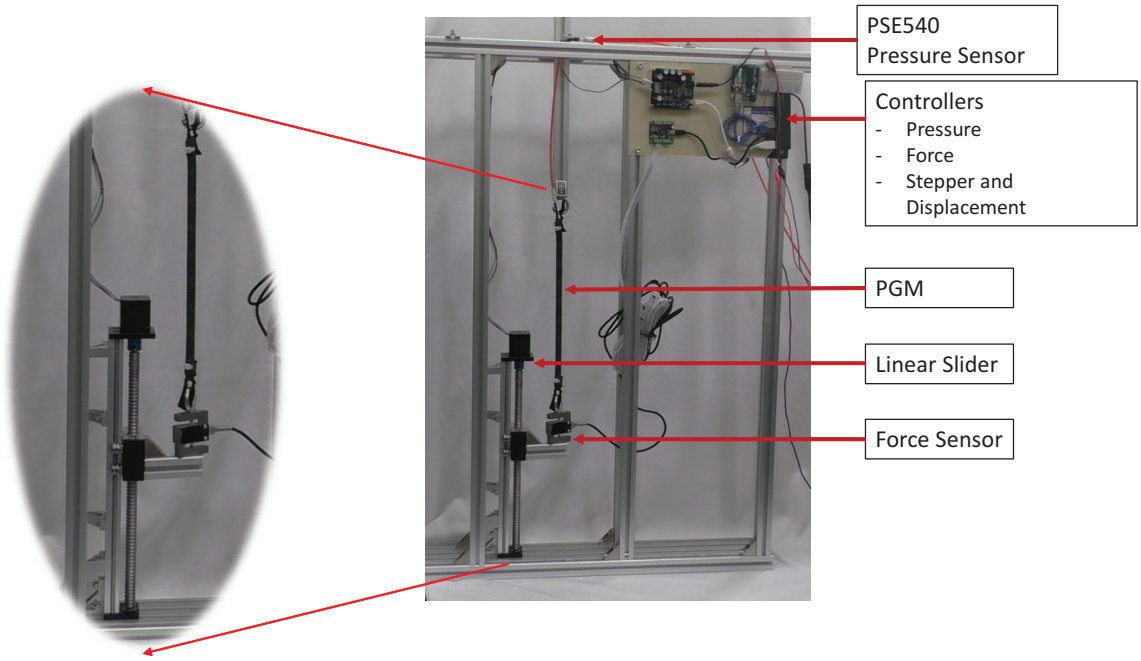

Fig. 2.5: Experiment apparatus developed to measure and model impedance characteristics of pneumatic gel muscles.

length, stepper motor with vertical torque limit of 10 kg (98.1N), s-type load cell with range of 0 - 100 kg range, pressure sensor PSE-540 with pressure range of 0 - 1 MPa. The phidget stepper controller is user for position control and logging, load cell and pressure values are recorded using Arduino and phidget load bridge. The synchronized sinusoidal motion was programmed in python and controlled though PC. Synchronized logs were collected and recorded for further analysis.

2.3.3 Impedance Model

We conducted two sets of experiments, first to measures force due to stiffness. This was done by hold a position until force remains unchanged at displacement of 5 mm starting from 0 position to elongation of 8 cm and contraction back to zero position. In second experiment we measured total force in dynamic experiment where PGM was made to oscillate at various maximum velocities for different air pressure. The measurement

recorded in the second experiment represents total force and subtracting force due to stiffness form total will give us damping force. Following equation is used to measure force due to damping effect.

$$F_d\left(P_m,\ \dot{x}\left(t\right)\right) = \ F\left(t\right) - \quad F_s\left(P_m,\ x\left(t\right)\right)$$

Surface fitting techniques and custom equation assumed in our model is used to identify stiffness and damping coefficients due to change in air pressure, displacement and velocity of actuation and change in position. We found that default assumed model is not enough for approximate model of force but requires air pressure dependent variable constants to prefect the model. Following equations describes the modeled stiffness and damping force of PGM in dynamic conditions. Table 2.1 shows values for model parameter considering working range of 100 kPa to 300 kPa and displacement velocity of 15 mm/sec to 60 mm/sec.

$$F_s = f\left(x,\ P_m\right) = \ \left(A_{10} + A_{11}P_m\right)\ x + A_{12}x$$

$$F_d = f\left(\dot{x},\ P_m\right) = \ \left(D_{10} + D_{11}P_m\right)\ \dot{x} + D_{12}x + D_{13}$$

Figure 2.6 and Figure 2.7 shows experiment data point and modeled surface for stiffness and damping force against pressure displacement and velocity of actuation. The residual plots show difference in experimental and modeled data. The R-square of stiffness model is 0.9805 whereas R-square for damping model is 0.6057.

Table 2.1: Modeled coefficients of stiffness and damping characteristics of pneumatic gel muscle using curve fitting methods.

A10	A11	A12	D10	D11	D12	D13
0.02982	0.001876	-0.01184	0.02071	-7.89E-05	0.003598	0.5606

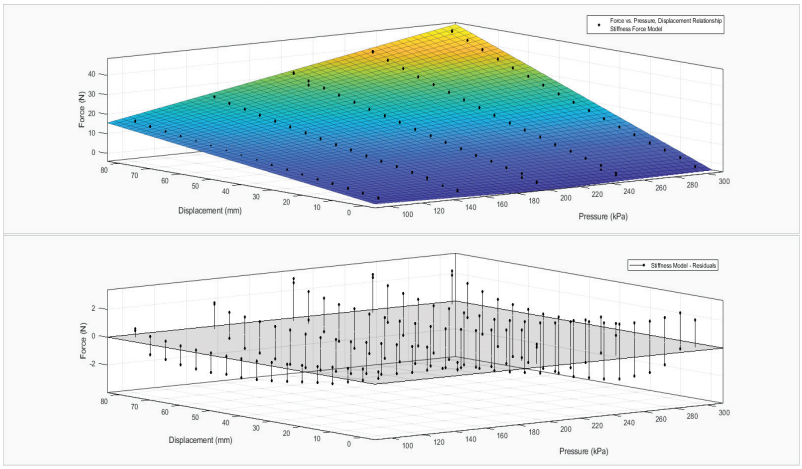

Fig. 2.6: Model realized for stiffness characteristics of pneumatic gel muscle measured during experiment.

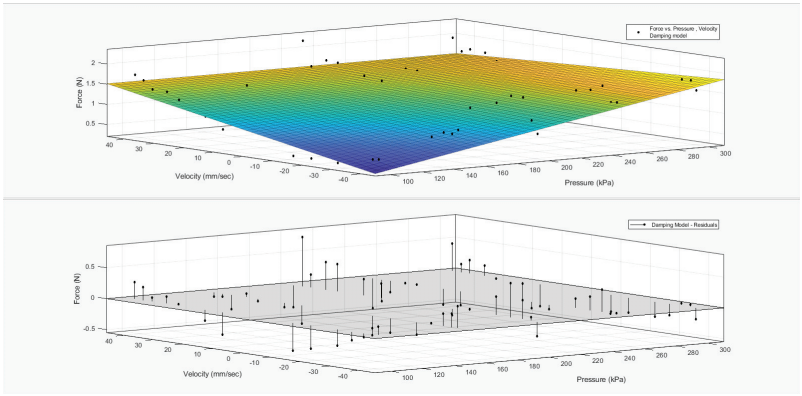

Fig. 2.7: Model realized for damping characteristics of pneumatic gel muscle measured during experiment.

2.3.4 Impedance Model Verification

The model identified above is simulated against the stiffness, damping and dynamic experiment data. The data shows results are closed to the measured force in all conditions. Figure 2.8 and Figure 2.9 shows relation and comparison of measured and modeled data for stiffness and damping forces for difference air pressure. Figure 2.10 shows the relation of displacement and velocity with measure force versus modeled force for dynamic total force generated by PGM.

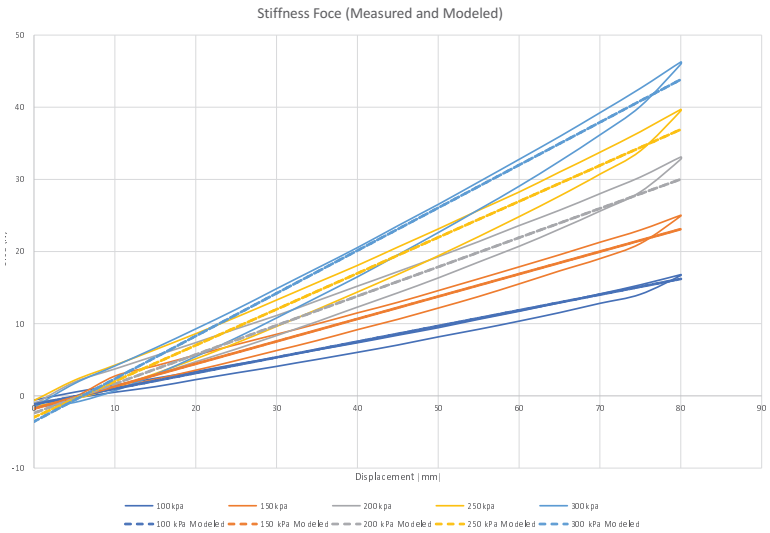

Fig. 2.8: Force due to stiffness measured during static experiment. The sold line graph shows measured data. The dotted lines graph shows modeled data.

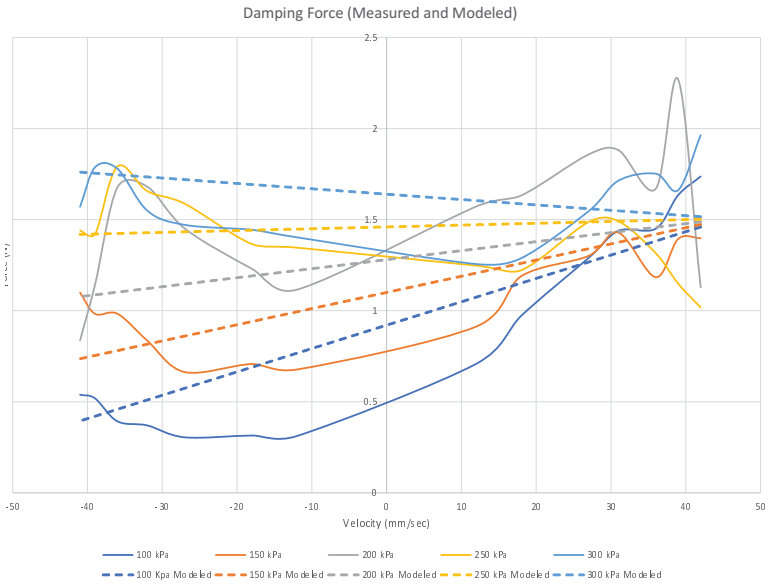

Fig. 2.9: Force due to damping calculated from dynamic experiment. The sold line graph shows measured data. The dotted lines graph shows modeled data.

From this data we observe that the model shows approximately close to the measured data. Damping effect are highly nonlinear and have only 60% accuracy. The

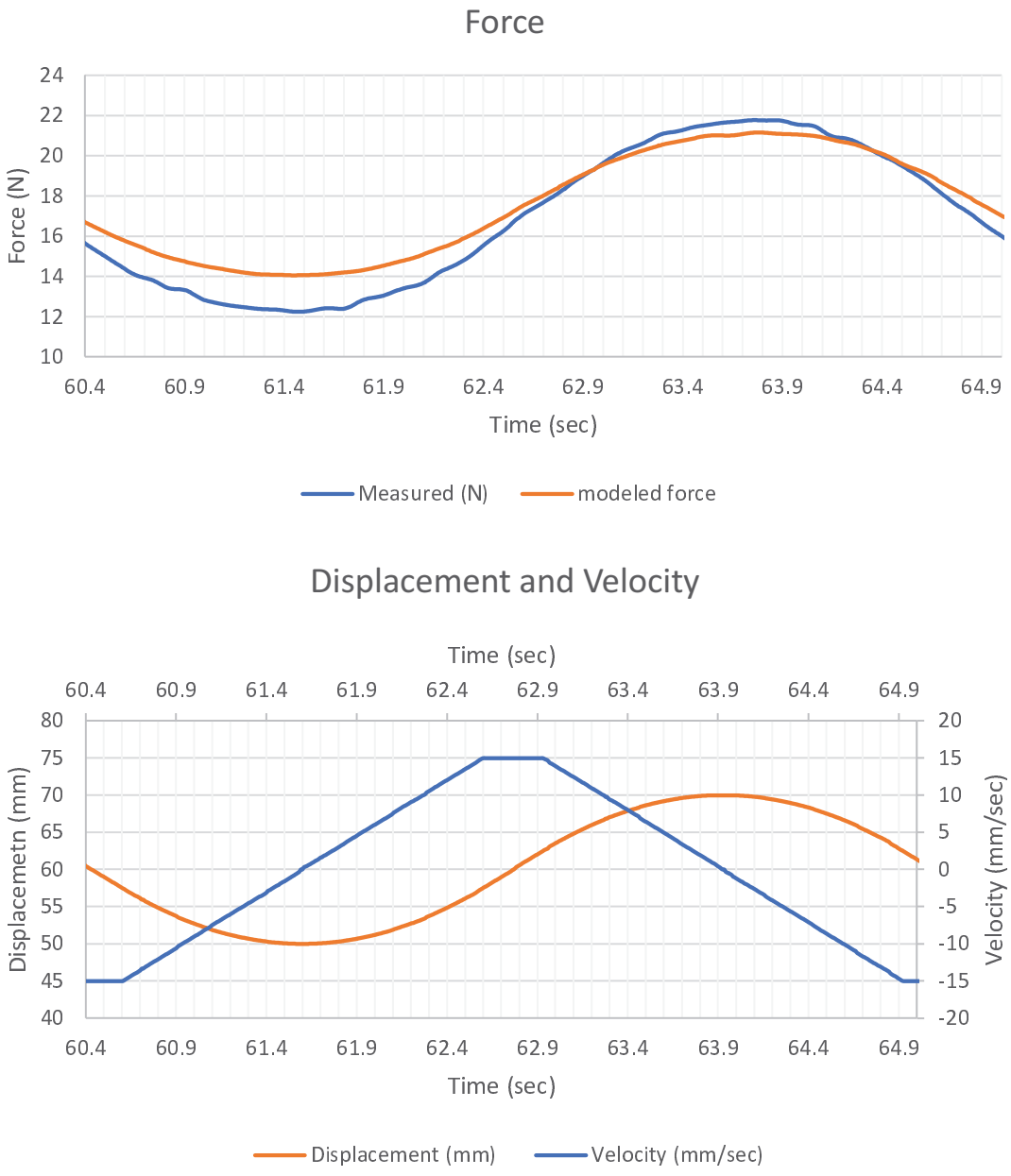

Fig. 2.10: Model verified at dynamic condition at 15 mm / sec max velocity of displacement showing less modeled force following trijectory of experimental force with difference of 2 N at the begenning of elongation.

total force is deviates by approximately 2N at the beginning of elongation where are gets accurate at full elongation.

We can now use this model to develop assist control algorithms for supply required torques or forces for respective velocity and displacement. This will make the device highly compliant to user motion and provide less distraction for dexterous human motion. In the following sections we will discuss the design of AWS and its control algorithms.

2.4 Assist Control Algorithms

In this section we will discuss stance and swing phase detection algorithm based on contralateral foot movements and two control algorithms based on using gait change event.

2.4.1 Gait Detection Algorithm

To reduce the muscle efforts during swing phase of the gait cycle we need to identify the beginning and end of the gait cycle. In our design this was done by using force sensitive resistors (FSR) in the shoe. The FSRs are places at the heel of the shoe as shown in Figure 2.11. The placement of the FSR is used for detecting stance phase of the gait cycle. Since the gait is synchronous activity of both limb when one limb is in the stance phase other limb is in the swing phase. The dual support phase during which transition between stance and swing happens, helps us identify the limb in swing phase using FSR sensors in the shoe. Based on this the system identifies which limb to assist and when to start and stop assist i.e. actuate PGM by controlling pneumatic solenoid valves operation.

This algorithm to detect gait cycle is continuous process of polling FSR sensor readings detecting gait phase and trigger assist control.

Fig. 2.11: FSR sensor fixed to heel portion of the shoe to detect stance phase of the gait cycle.

$$f(PGM_{actuation}) = f(R, L) \tag{2.1}$$

where $f(PGM_{actuation})$ is actuation control function which depends on $R = f(R_{fsr})$ and $L = f(L_{fsr})$ which are functions of FSR sensor in right and left limb respectively. FSR_{ref} is reference value of FSR sensor used for distinguishing between stance and swing phase while walking.

R and L are defined as follows

$$R = \begin{cases} 1, & \text{if } f(R_{fsr}) \geq FSR_{ref}, \text{ i.e. Stance Phase} \\ 0 & \text{otherwise, i.e. Swing Phase} \end{cases} \tag{2.2}$$

$$L = \begin{cases} 1, & \text{if } f(L_{fsr}) \geq FSR_{ref}, \text{ i.e. Stance Phase} \\ 0, & \text{otherwise, i.e. Swing Phase} \end{cases} \tag{2.3}$$

From Eq 2.2 and Eq 2.3 we can clearly identify the present phase of the respective limb. Based on this we update Eq 2.1 as follows:

$$f(PGM_{actuation}) = \begin{cases} L_{assist}, & \text{if } R = 1 \ \& \ L = 0 \\ R_{assist}, & \text{if } R = 0 \ \& \ L = 1 \\ \text{No Assist}, & \text{otherwise} \end{cases} \tag{2.4}$$

$$f(PGM_{actuation})$$

in our study is derived by two methods first is simple feed forward control where magnitude os assistive force is defined by user and adaptive assist control where magnitude of assist control is decided based on speed of walking. These methods are explained in following sections.

2.4.2 Feed Forward Assist Control

Figure 2.12 shows the control mechanism of the AWS with the FSR-406 sensor based stance and swing phase detection mechanism and assistive control. It is a continuous process of proportional (P) control where an Arduino Uno board monitors the FSR sensor data to identify the limbs in the stance and swing phase in the gait cycle. Detection of the limb in the swing phase triggers the assistive control mechanism of the PGM. For actuation control, we used a Kaganei G010E1 3/2 normally closed solenoid valve. The FSR sensor data are continuously monitored for switching ON/OFF solenoid valves. This system is realized using following equation

$$E = RY$$

$$U = kpE$$

where E is error signal, R is the calibrated threshold value of the FSR sensor, Y is the analog value of the FSR sensor, U is the input to the solenoid valve, and kp is the

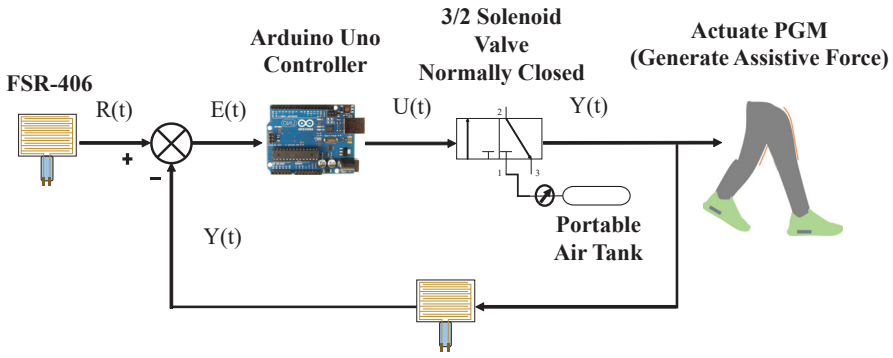

Fig. 2.12: Feed forward control of augmented walking suit

P-gain. The assistive control mechanism detects the gait cycle by sensing the transition from one phase to another on both limbs in DLS. This way, we avoid unwanted assistive forces during the stationary state where there is no transition. The assistive force generated by the AWS is directly proportional to the supplied air pressure. The supplied air pressure is controlled using the regulator attached to a small air tank used as a source of air pressure.

In the flowchart described in Figure 2.13 FSR sensors in both limbs are used to detect gait cycle, i.e., to identify if the user is walking. Upon detecting the gait cycle the algorithm identifies the limb in the swing phase and actuates PGM actuator to provide the assistive force by turning on pneumatic solenoid valve.

2.5 Augmented Walking Suit

2.5.1 Introduction

The UPS designed in previous studies requires no electricity but uses the walking motion to power the PGM with the help of a pump in the shoe. The evaluation of the UPS shows that it reduces the muscle efforts in the swing phase of the gait cycle. However, the effect is invisible for all the muscles of the lower limb owing to a small amount of assistive force generated. For better performance, the use of external power

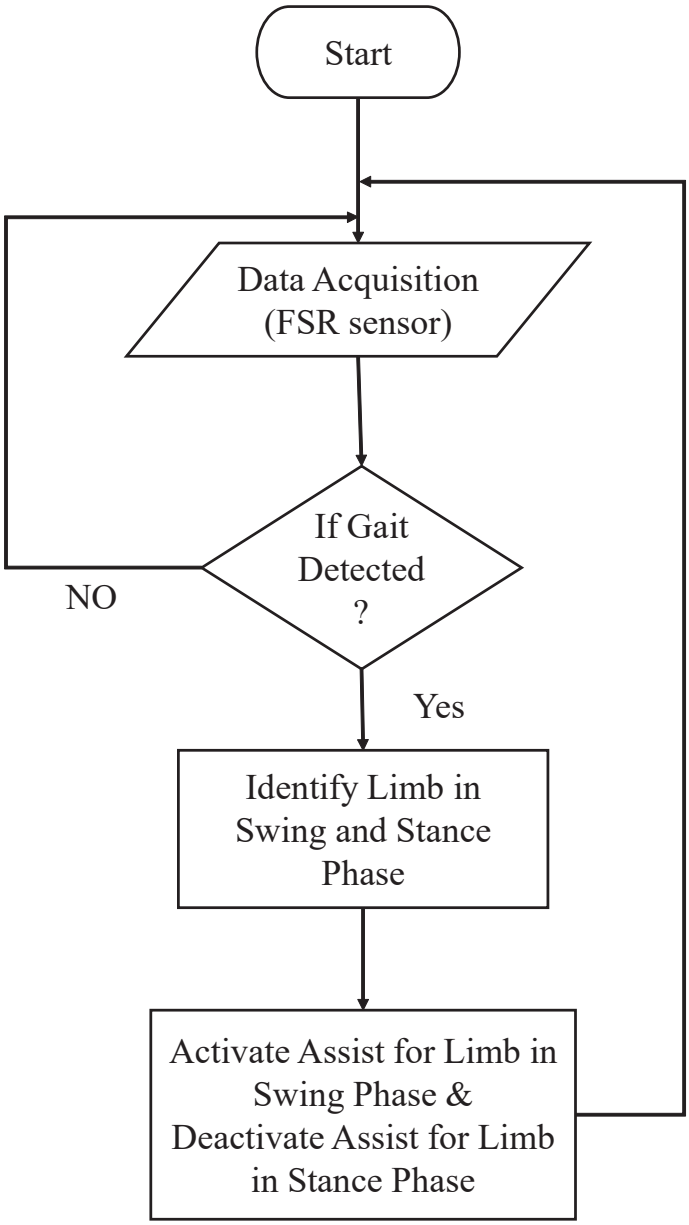

Fig. 2.13: Flow chart of PGM actuation logic for generating assistive force.

sources such as an air tank and a pneumatic valve control can enhance the augmentation factor of the assistive suit.

To prove this hypothesis, we conducted experiment to examine and distinguish the PGM actuation delay for the pump and the air tank as a source of air pressure, by

Table 2.2: Specifications of sensors used in the experiment

Category	Sensor Name	Specification
Air Flow Rate Sensor	PFMV-530-1	0-+3.0 L/min
Air Pressure Sensor	PSE540-1M5	0-1Mpa
Loadcell force sensor	CZL653	0-200N
PhidgetBridge	1046_0B	

recording the air pressure, air flow rate, and force-generation with respect to time. The objective of this experiment was to identify the difference in the time when the air pressure is supplied to when the PGM generates the force. Figure 2.14 shows the experimental setup; it consists of a PGM with both ends hooked up with one end attached to the Phidgets loadcell to record generated force, the air pressure sensor at the inlet valve of the PGM, and the air flow sensor to record the air flow rate at various air pressures. Table 2.2 lists the specifications of the sensor. In this experiment, we used a rubber pump and a portable air tank to actuate the PGM. The delay was recorded for two PGM configurations, first when the PGM is attached at its rest length and second when the PGM is stretched to 370 mm. The graphs in Figure 2.15 and Figure 2.16 show the actuation delay profiles of the PGM for the air sources of pump and air tank. We observed that when the pump is used, the delay in the generated force is approximately 260 ms and 130 ms for the rest length of 300 mm and the stretched length of 370 mm, respectively. However, when the air tank is used as a source, no delay is observed between the supplied air pressure and generated force.

Based on this observation, we found that for the UPS, generating the assistive force precisely is difficult owing to the delay and the difficulty in attaching multiple pumps in the shoe, which also disturbs normal walking. Therefore, we developed a PGM actuation control based on the gait detection system that can benefit and elevate the performance of the walking assist suit. In the next section, we discuss the design and

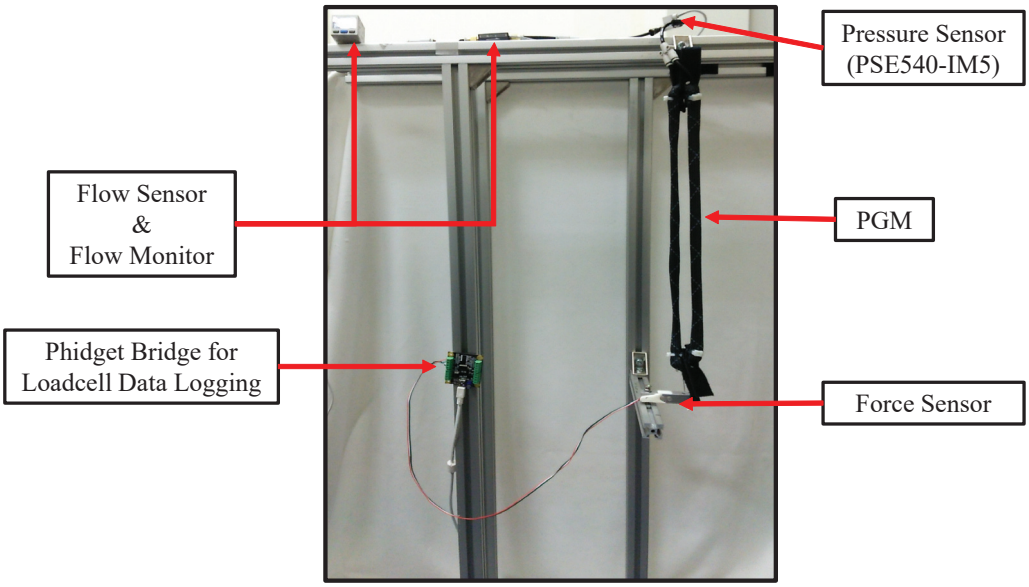

Fig. 2.14: Experiment setup to measure actuation delay of rubber pump and portable air tank used as air pressure source.

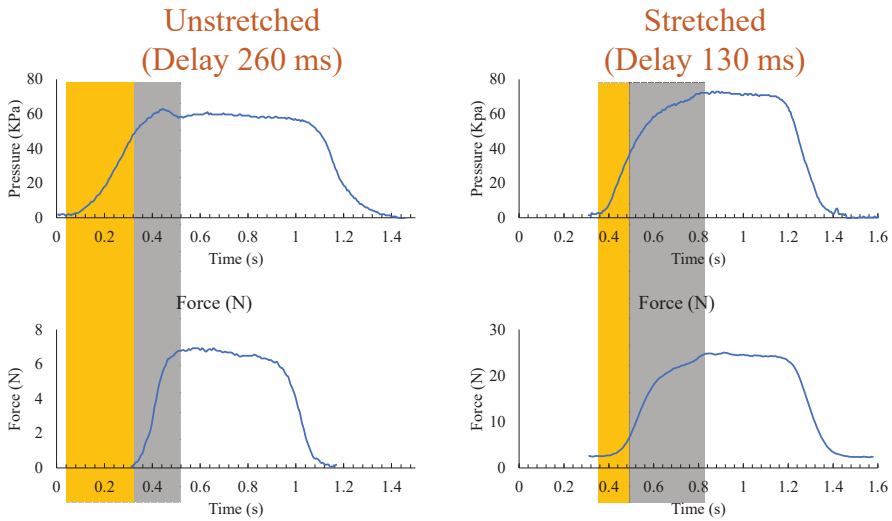

Fig. 2.15: Actuation delay caused when the pump is used as the air pressure source. The first row shows the generated air pressure and the second row shows the generated force with respect to time.

control of a newly developed walking assist suit.

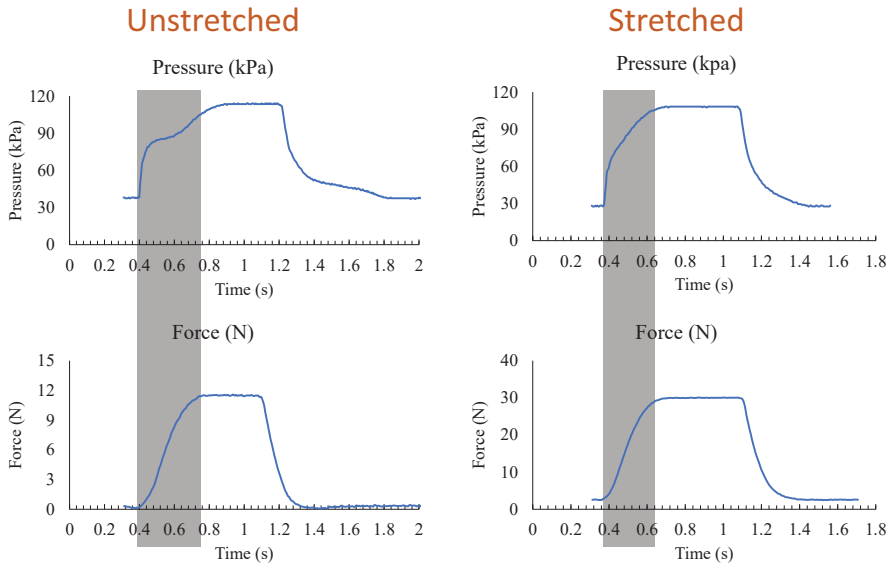

Fig. 2.16: Actuation delay caused when the tank is used as the air pressure source. The first row shows the generated air pressure and the second row shows the generated force with respect to time.

2.5.2 Design of Augmented Walking Suit

To overcome the challenge of the UPS, we developed a new walking assist suit called the AWS. AWS is developed based on the principle of the UPS, i.e., a lightweight, wearable, low-powered assistive suit. For the AWS, pneumatic solenoid valves are used for the actuation control of the PGM to generate the assistive force, and the control signal was derived based on the gait detection system developed using pressure sensors in the shoes. The new design enables it to support a walking pitch of more than two steps per second which was not possible in UPS [14] and the level of augmentation can be controlled by setting the maximum supply air pressure. K. Ogawa et al. mentioned that the maximum air pressure that the PGM can handle is 300 kPa, and contraction ratio increases with the air pressure. Therefore, setting the maximum cutoff air pressure using a pressure regulator decides the augmentation factor of the suit during walking.

The AWS consists of a waist support, a knee support, PGMs attached along the quadriceps femoris, pressure sensors, pneumatic solenoid valves, controllers, and a portable air tank. Figure. 2.17 and Figure. 2.18 show the overview and illustration of the applied assistive force during the swing phase of the gait cycle. Figure.2.17 shows that the PGM is attached along the thigh muscles with the help of the waist support and knee support, while the backpack contains the controller circuit, the portable air tank, and a battery for the controller, and the pressure sensors in the shoe are connected to the controller. Figure. 2.18 illustrates the applied assistive force; the elastic nature of the PGM allows it to stretch during the stance and terminal stance phases and from the terminal stance controller that actuates the PGM for the swing phase of the gait cycle.

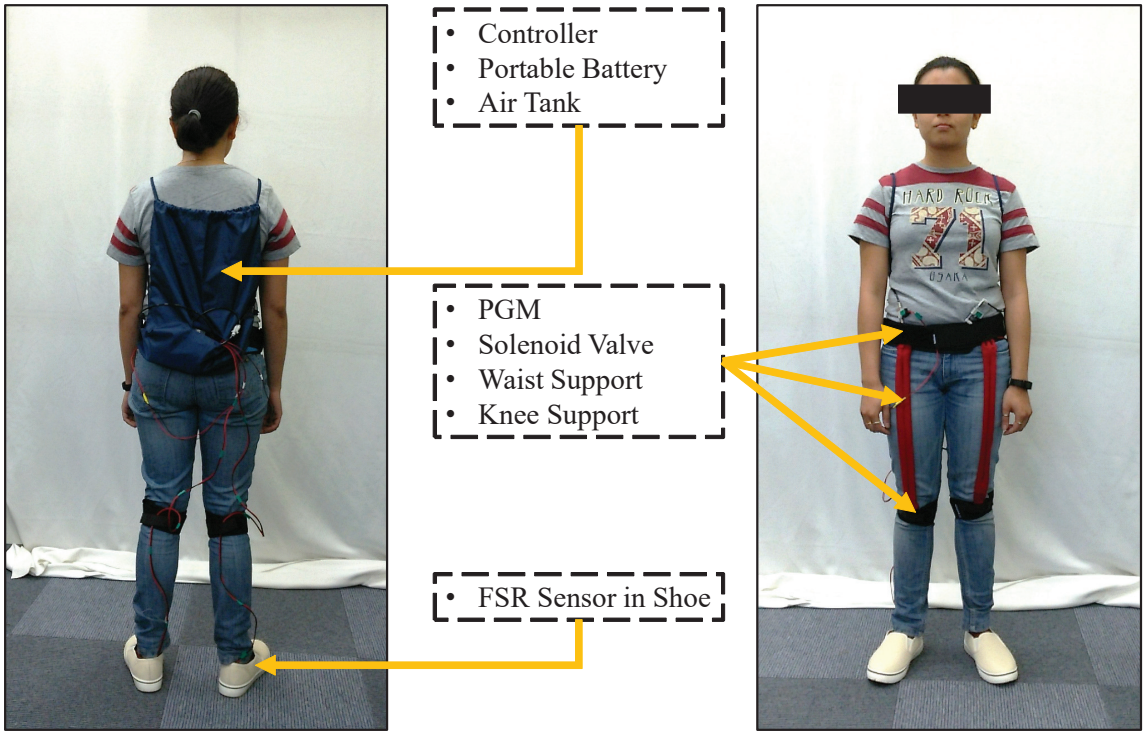

Fig. 2.17: AWS Design and Construction

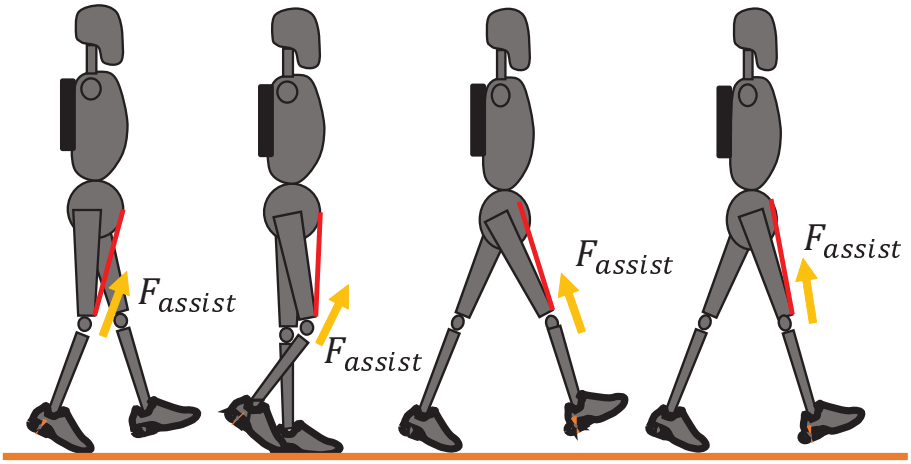

Fig. 2.18: Applied assistive force during swing phase of the gait cycle supporting forward locomotion

Table 2.3 lists all the components of the AWS with respective specification and weights. Based on this total weight of AWS is 2 kg approximately , the battery lasts for 3-4 days of runtime and the air tank can actuate 500 actuation at 100 kPa when tested in the lab.

Table 2.3: Components of the AWS, their specification and weights in kilogram.

Name	**Quantity**	**Specification**	**Weight (kg)**
Air tank	1	40 (liters)	0.3
Regulator	1	0 - 0.5 Mpa)	0.34
PGM	2	30 cm	0.11
Tubes	1	Polyurethane (4 mm)	0.022
Knee Support	2	Fabric	0.052
Waist Support	1	Fabric	0.11
Controller	1	Arduino Uno	0.3
Battery	1	10000 mAh / 38.48 watts	0.24
Backpack	1		5
Total Weight of AWS			1.974

The AWS uses the PGMs along the quadriceps femoris muscles connected across two

joints: the pelvis and the knee. This configuration provides the assistive force during the swing phase of the gait cycle, and reduces the muscle effort of the quadriceps femoris during the swing phase of the gait cycle. The air pressure supply is controlled using the pneumatic solenoid valve. We also developed a gait detection system that identifies the swing phase of the individual limb. This system consists of two FSR-406 pressure sensors placed in each shoe. These are used together to detect the walking motion, standing posture, and gait cycle of the individual limb, and identify the phase of the gait cycle.

2.6 Conclusion

In this section we talked about human gait cycle in detail with classified the gait cycle based on foot orientation and task performed. The mathematical model of timing and major gait phases and dual support phase was defined. Based on this concept we defined gait detection algorithm using FSR sensor in the shoe to detect stance phase of the gait cycle and differentiate between the phase of both limbs while walking. The algorithm was the implemented in augmented walking suit for providing assist to move forward while swing phase of the gait cycle. Now in the following section we will discuss the evaluation of AWS by measuring surface EMG (sEMG) and kinematics of lower limbs.

Chapter 3

Evaluation of Augmented Walking Suit

3.1 Introduction

To test our assumption that the newly developed AWS can assist walking and that change in assistive air pressure reduces muscle activity in lower-limb muscle groups the experiment was conducted to test the performance evaluation of the AWS with two levels of assistive air pressure.

Walking involves a combination of muscle activation dynamics of the anterior and posterior lower limb muscles. These changes were recorded using sEMG signals of eight major posterior and anterior muscles that contribute to the gait cycle. We measured TA, SOL, MG, LG, RF, VM, VL, and BF. These muscles are superficially accessible to record sEMG of the lower limb and collectively support the gait cycle. The performance of the AWS is measured based on the statistical difference in the sEMG recorded when the subject was not wearing the AWS and wearing the AWS with two levels of assistive air pressure.

3.2 sEMG Based Evaluation

3.2.1 Experiment Method

To evaluate the effect of the AWS on the muscle activation pattern of lower-limb muscles for two levels of assistive air pressure, the device was tested on a group of seven healthy young subjects with no gait abnormalities. The subjects age (± SD) was 28.8 ± 5.1, height was 150 ± 10 cm, and weight was 70.8 ± 14.5 kg. All the subjects participated in the experiment after a brief introduction of the AWS and experiment requirements.

For effective evaluation of the assisted gait, we need to measure a minimum of three full gait cycles [22]. In our experiment, we recorded sEMG for ten full gait cycles. This was done by asking subjects to walk 15 m straight on a flat surface by maintaining the walking speed during all experiments. The sEMG and FSR sensor data were logged using Personal EMG (P-EMG) device from Oisaka electronic Ltd. For continuous and uninterrupted walking and recording of the data during the experiment, we prepared a backpack containing the P-EMG device, portable battery, and a laptop to operate the P-EMG device. The backpack also contained a controller circuit for the AWS and portable air tank. The laptop was accessed remotely to record the sEMG. Figure. 3.1 shows the experimental setup with the backpack. The total weight of the backpack during experimental evaluation was 6 kg. Before starting the experiment, we recorded MVC for each muscle under observation for all subjects. Exercises such as squat for BF; calf raises for SOL, LG, and MG; thigh contraction for RF, VM, and VL; and ankle dorsiflexion for TA are used to record MVC.

With the above setup, we conducted three experiments to evaluate the AWS. In the first, sEMG data were recorded for a normal gait, i.e., when subjects were not wearing the AWS. This data gave us the baseline for evaluating the effects of the AWS. In the second and third experiments, sEMG data were recorded for the assisted gait, i.e.,

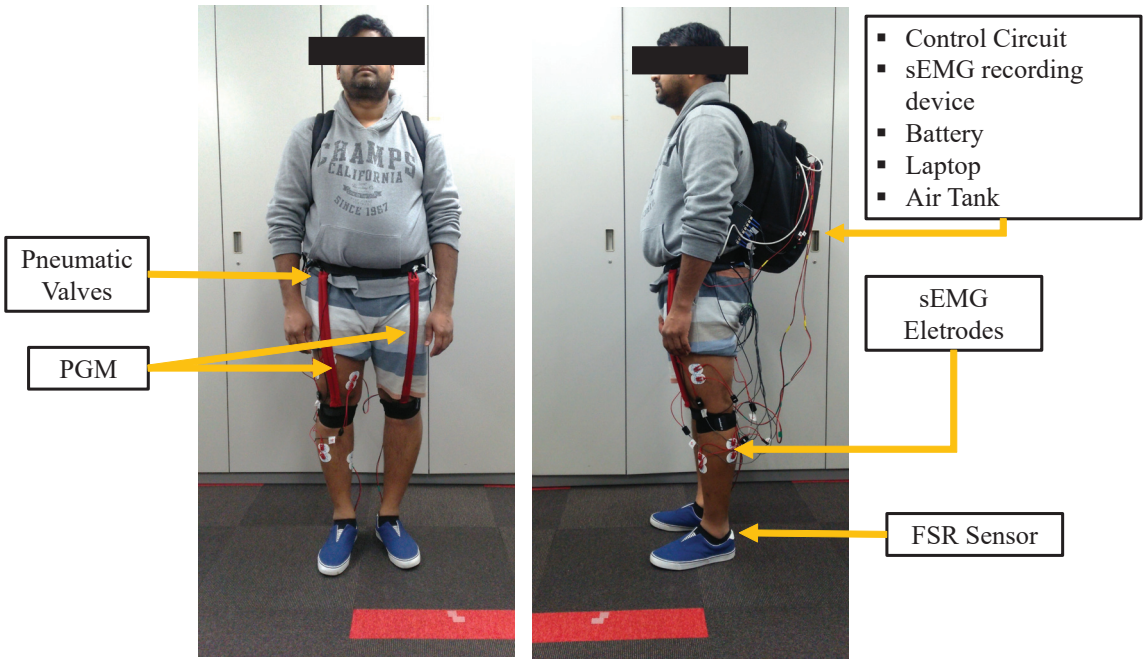

Fig. 3.1: Experiment setup, subject wearing AWS, electrodes and backpack. The backpack contains sEMG recording device, laptop, controller for the AWS, portable battery for controller and sEMG recording device. The total weight of the backpack is 6 kg.

subjects wearing the AWS with the backpack containing the experimental setup. For all subjects sEMG of right limb was measured for two levels of assistive air pressure during this experiment, i.e. 60 kPa and 100 kPa respectively. Three iterations of each experiment were performed to record enough data to conduct a statistical analysis.

3.2.2 Results

The recorded sEMG was rectified with integrated EMG (iEMG), a second-order low-pass filter with a cut-off frequency of 100 Hz, and a second-order high-pass filter with a cut-off frequency of 40 Hz using the P-EMG plus tool for the P-EMG device. The recorded sEMG was normalized using MVC to find %MVC, and ten gait cycles for each subject were averaged to create one gait cycle which is further averaged to generate one gait cycle of all subject. The segmentation of gait cycle was done from stance to

stance detection on the left limb based on FSR sensor data in P-EMG tool. This was done because stance phase of one limb assists swing phase of the contralateral limb. We measured standard deviation and performed statistical analysis using a two-sample t-test on the average normalized sEMG for all muscles under observation.

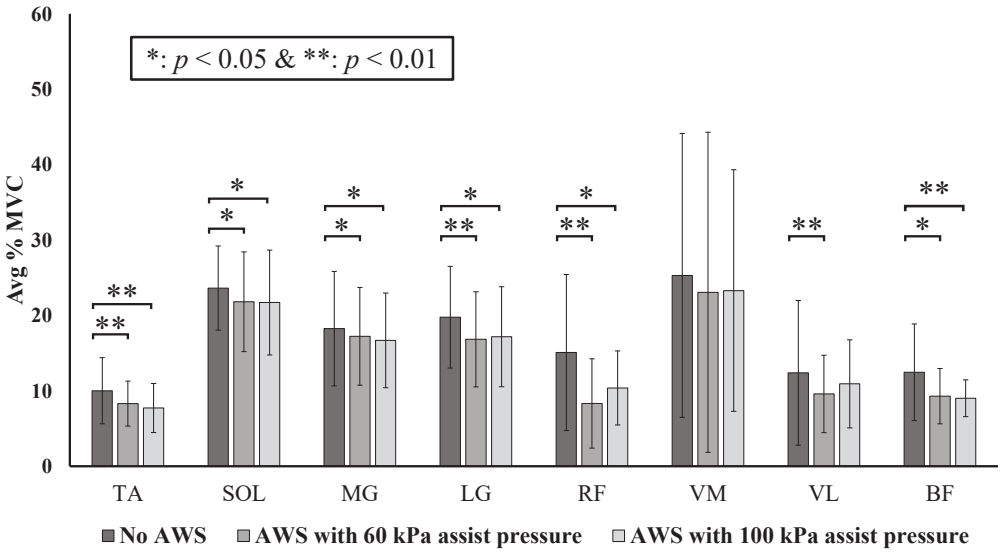

Fig. 3.2: The figure shows the significance of the reduction in %MVC of the muscle groups for unassisted and assisted with two level of assistive force. The result shows significant reduction or no change in the muscle activation during assisted walking recorded for seven subjects.

Figure 3.3 shows the normalized average sEMG signal envelope for all subjects with standard deviation of the gait cycle without wearing AWS and wearing AWS with two levels assistive air pressure at 60 kPa and 100 kPa. The gait cycle reference for the sEMG signal is swing to swing phase of the right limb.The figure also shows the FSR sensor data for both limbs. The signal peak shows the stance phase on the respective limb and swing on the contralateral limb. AWS detects stance phase on the left and assists swing phase of the right limb (during the experiment we measured sEMG of the right limb). From the graphs, we see that, as we increase the assistive air pressure reduction in the peak value of the normalized averaged sEMG signal not only in the

swing phase but also in the stance phase. To evaluate the differences quantitatively, we conducted a two-sample t-test between unassisted gait when AWS was not worn and assisted gaits. Figure. 3.2 shows averaged %MVC for the three experiments and their significance for individual muscles.

Table 3.1: Result of two sample t-test with the respective p-value, t-value and t-critical. P-values are marked with * (< 0.05) or ** (< 0.01) as displayed in Figure 3.2.

Muscles	**Experiment**	***p-value***	***t-value***	***t-critical***
TA	AWS 60 Kpa	0.0001 **	14.51	2.78
	AWS 100 Kpa	0.0002 **	24.25	3.18
SOL	AWS 60 Kpa	0.0392 *	3.02	2.78
	AWS 100 Kpa	0.0329 *	3.20	2.78
MG	AWS 60 Kpa	0.0310 *	3.85	3.18
	AWS 100 Kpa	0.0116 *	4.41	2.78
LG	AWS 60 Kpa	0.0095 **	4.68	2.78
	AWS 100 Kpa	0.0201 *	4.53	3.18
RF	AWS 60 Kpa	0.0079 **	6.35	3.18
	AWS 100 Kpa	0.0420 *	4.72	4.30
VM	AWS 60 Kpa	0.0670	2.50	2.78
	AWS 100 Kpa	0.3300	1.16	3.18
VL	AWS 60 Kpa	0.0075 **	6.46	3.18
	AWS 100 Kpa	0.4003	1.06	4.30
BF	AWS 60 Kpa	0.0192 *	7.11	4.30
	AWS 100 Kpa	0.0020 **	10.16	3.18

All the muscles showed significant reduction or no change in the muscle activity evaluated during the experiment. Muscles showed reduction for both levels of assistive air pressure. Table 3.1 shows the result of the two-sample t-test showing the significance of the reduction in the muscle activity based on $p - value$. The Table 3.2 shows percentage reduction in muscle activity. TA, LG, RF, VL and BF shows larger reduction in %MVC while for SOL, MG and VM shows reduction less than 10% of %MVC. From the data in both the tables we observe that assisting swing phase by controlled actuation reduces muscle activity of the measured muscles of the lower limb.

Table 3.2: Reduction average of % MVC compared with normal gait. $-ve$ value indicates the increased in % MVC, $+ve$ value represents the decrease in % MVC.

Muscle	**AWGAS no assist % of Normal Gait**	**AWGAS assist % of Normal Gait**
TA	14.73	17.55
SOL	-8.69	6.76
MG	13.11	6.80
LG	22.39	8.87
RF	38.41	33.15
VM	7.65	13.13
VL	21.77	20.18
BF	34.00	31.04

Therefore, based on the results and analysis we found that the AWS developed in this study can augment human gait as compared to when no AWS is worn. The AWS was able to reduce the muscle efforts significantly in both levels of assisted by assisting swing phase of the gait cycle.

3.3 Conclusion

Our results show that the previously developed PGM can be used for the development of the AWS and make it lightweight, portable, and easy to use. The use of the AWS showed a reduction in the muscle activity in all the major lower-limb muscles. Because of the soft nature of the suit this device does not drastically disturb the normal gait of the wearer.

The assistive control developed for the AWS detects limbs going in the stance and swing phase during DLS by sensing the FSR sensor data. The simple P control supports 20%-30% of the gait cycle during the swing phase. Because of the nature of the gait cycle and power source for the actuator, it is easy to add additional PGMs to the AWS for increasing the range of the assistive force. It is also possible to support the

stance and swing phase on a contralateral limb using same solenoid valve, since in the standard gait cycle both limbs functions synchronously. The device uses waist and knee support to attach the PGM along the rectus femoris muscle. This position sometimes a causes little disturbance during walking. It can be addressed by changing the way PGMs are attached to the limbs in such a way such that it does not disturb the degree of freedom at the knee or any other joint when the PGMs are used.

State-of-the-art wearable walking assist suits are inspired by the biological function of walking, and the assistive actuators aligned with the muscles and joints of the lower limb. In such devices, the swing phase of the gait is assisted with an actuators attached close to the ankle or along the soleus muscle and a reduction in the metabolic cost of walking is demonstrated. In our research, AWS is developed to assist the swing phase PGM is attached along the RF muscle from hip to knee, and experimental evaluation shows a progressive reduction in the muscle activity of TA, SOL, MG, and LG. Along with this, RF, VL, and BF also show a reduction in muscle activity.

Qualitatively, from the oral feedback from subjects, we found that the device is lightweight when not using the 6 kg experimental setup; subjects also reported feeling the assistive force of the PGM during the swing phase of the gait cycle. Some subjects reported feeling assistive force during walking when assistive air pressure changed to 100 kPa as compared to 60 kPa. They also reported that the PGM attachments do not disturb the walking experience but improving the attachment at the knee can result in a more comfortable walking experience.

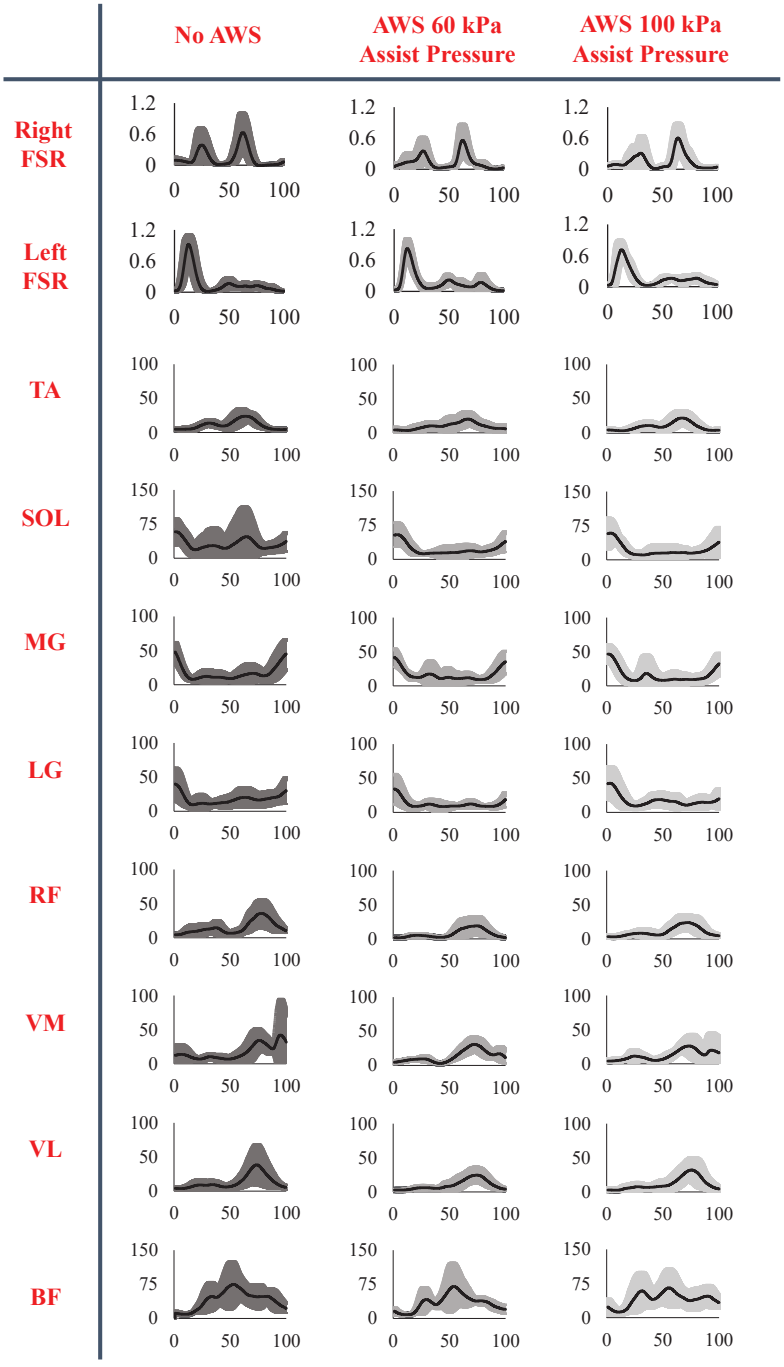

Fig. 3.3: The figure shows normalized averaged sEMG signal envelope for lower limb muscle groups observed for walking when AWS is not worn and when AWS is worn with two levels of assistive air pressure. It also shows FSR sensor signal showing assistive phase in the gait cycle. The X-axis is the percentage gait cycle (heel strike to heel strike). The Y-axis of the FSR signal is voltage out recorded on the P-EMG device, and for the muscle group, it is average percentage MVC recorded during the experiment.

Chapter 4

User Adoption Case Study and Pilot Trial

4.1 Introduction

Aging impacts muscle function and reduces ones ability to perform daily tasks comfortably. Elderly people face various challenges due to such condition to continue perform their work. Elderly farmers or workers are often expose to accidents or muscle injuries due to stressful work condition and can easily get tired. Elderly people find it difficult to use or adapt current set of human augmentation devices mainly due to the size, weight and ability to use it in agricultural environment. Previously developed a soft wearable and lightweight augmented walking suit (AWS) assists swing phase of the walking gait. Evaluation showed reduced muscle efforts and no major change in gait kinematics. To understand the requirement, usability and usefulness of the AWS in real life situation we conducted survey and pilot trial with farmers in rural areas. In this paper we discussed the feedback and requirements received through survey and pilot trials. The survey and subjective evaluation from these trials suggests the elderly people prefers lightweight and wearable assistive devices to reduce the required muscle efforts of similar tasks. [23] Quality of life and aging gracefully is directly linked with ones ability to easily performs his daily routine tasks.In 2018, Japans elderly popula-

tion was 28% of the total population [23] out of which 79% and 56% of elderly in the age group of 60 to 64 and 65 to 69 are engaged in work respectively [24]. As per japan industrial safety and health association (JISHA) [25] 25% of all the critical accidents involves people aged 60 and above. Most common reason for such accidents is occupational injuries, weak muscle or related to workspace management. To address these concerns researchers developed augmentation devices such as exoskeletons or exosuits for agricultural assistance or factory worker assistance devices [26] [27] [28] [29]. Human augmentation devices are developed to enhance ones physical ability to perform certain tasks. Exoskeletons greatly augment human ability, exosuits address wearability of exoskeletons and yet augments human motions it is designed for. The third category is assistive suit which uses wearable design and soft wearable actuators for human augmentation. These assistive suit augments human motion by reducing required muscle effort for certain tasks.

These recent advancement in the exoskeleton technology allows people working in factories and warehouses reduce stress and muscle fatigue. Yet, elderly find it difficult to use such devices mainly due to size and weight of such devices. Development of lightweight and wearable and easy to use devices is essential for elderly people involve in work.

To address one such concern about walking augmentation, herein in section 2, we briefly discuss the previously developed augmented walking suit (AWS) and its effect in the muscle activation pattern during walking. In section 3, we discuss the outcomes of survey and pilot trials conducted with farmers in rural area. The results, conclusion and future work involves are discussed in the following sections.

4.2 Overview of Pilot Trials

The objective of the pilot trial was to study the effectiveness, suitability, usefulness and improvements required for AWS to be used as wearable assistive device for elderly and others. Figure 2 illustrate overview of pilot study and expected outcome.

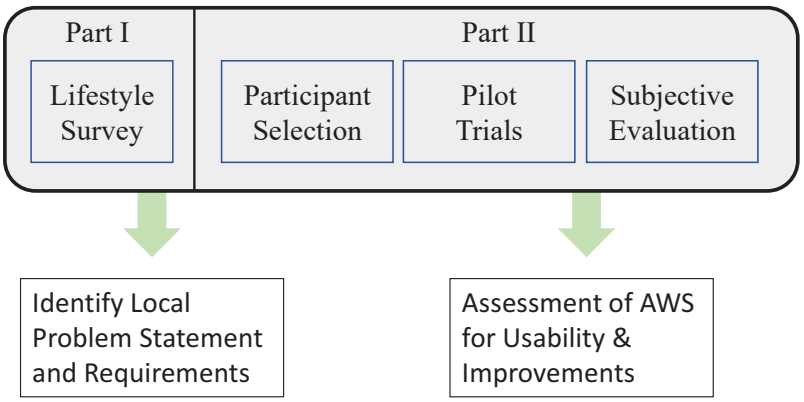

Fig. 4.1: Overview of pilot study and expected outcome

As shown in Figure 4.1 , this study was conducted in two parts, in first part we conducted survey about the lifestyle and problem faced due to health issues in agricultural activities. In second part, information related to AWS and its evaluation results, contents of the experiment and its objective were shared with the various prospective participants in the rural region including young and elderly.

4.3 Methodology

4.3.1 Survey and Data Analysis

The survey was distributed through the leader of various settlements in the rural areas. Each settlement includes 10 to 15 household. Total 63 people responded to our survey, average age of respondents was 65.31 (min=28 and max=85) and 95% were farmers. The survey targeted to identify the nature of work, agricultural practice, common prob-

lems faced during farming, are they open to use of assistive devices such as exoskeletons or wearable suit and their view on such technologies. Figure 4.2 shows physical limitation or problem faced during farming activity and Figure 4.3 shows various factors that might affect for adopting to assistive devices. It shows 21% face difficulty or fatigue in their upper limb, 11% face back pain, 17% faces stress in legs and 40% said whole body pain. From Figure 4.3 we also observed that most people would want to use newer assistive devices such as exoskeleton or assistive suit provided they are easy to use, safe and affordable. For some respondents its weight and portability is important for adopting to such devices.

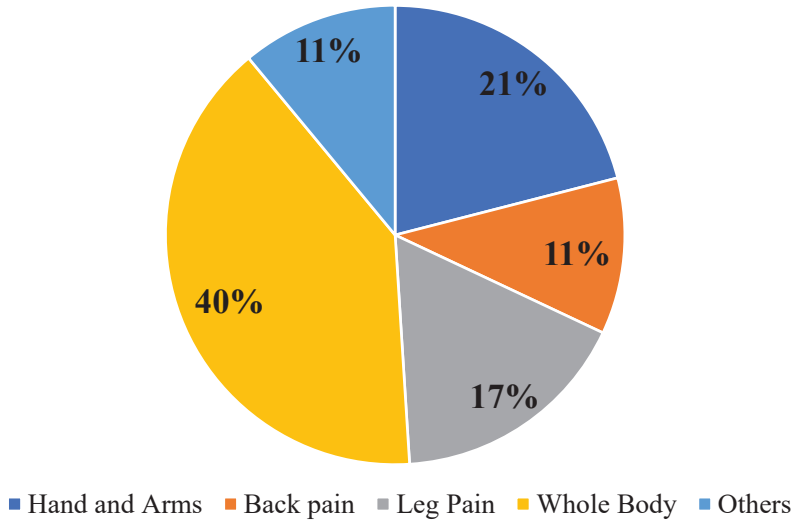

Fig. 4.2: Survery results showing problem faced by people in rural area.

4.3.2 Pilot Trials

We decided to conduct pilot trials with voluntary participants to get genuine feedback. To do this we prepare proposal with objective of the study, information about AWS outcome of lab experiments and methods to conduct pilot trials. We plan to conduct trials at the workspace of respective participants. Four people agreed to participated

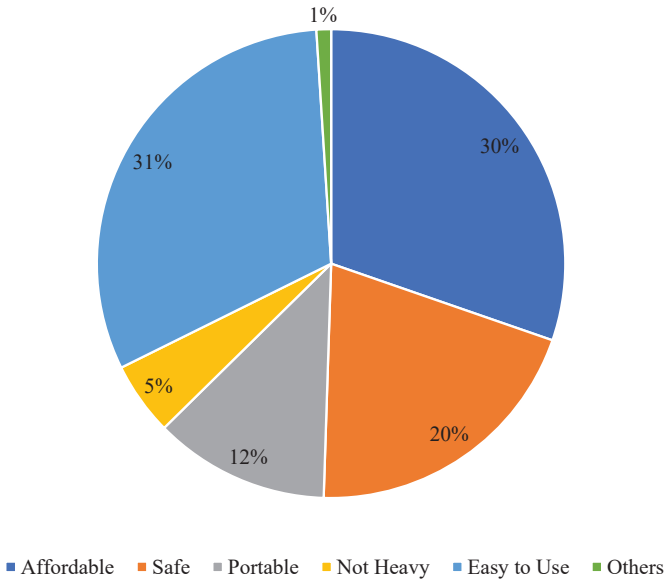

Fig. 4.3: Key factors responsible for adapting assistive suits in rural areas

in our study. All four with different age, sex and agricultural practice.

First trial was conducted with young female farmer at her rice field. Her work involves maintenance of poultry farm and rice field and all the related work. The second trial conducted with elderly farmer whos work involves organic rice and vegetable farming. The third trial conducted with two young farmer whos work involves rice farming from growing seedlings to processing and packaging rice. Figure 4.4 and Figure 4.5 shows volunteers wearing AWS and elderly farmer testing it while performing various activities near his workplace respectively.

4.4 Results

After AWS trials, feedback from all the participants were collected using questionnaire and open-ended interview. Figure 4.6 shows important aspect from questionnaire. The answer to the question is in the range of 1 to 5, where 1 is least likely and 5 is highly

Fig. 4.4: Volunteers trying to AWS.

Fig. 4.5: Elderly famer trying AWS performing various daily farming related activities.

likely. From these feedbacks we observed that participants could feel the assistance during walking, it did not interfere regular tasks and was comfortable to walk and they can differentiate between walking with and without assistive suit. All participants feel the suit is not heavy and moderately easy to use.

From open-ended interview with each volunteer after trial all said, walking with AWS feels easy as compared to without AWS. The suit is lightweight and does not

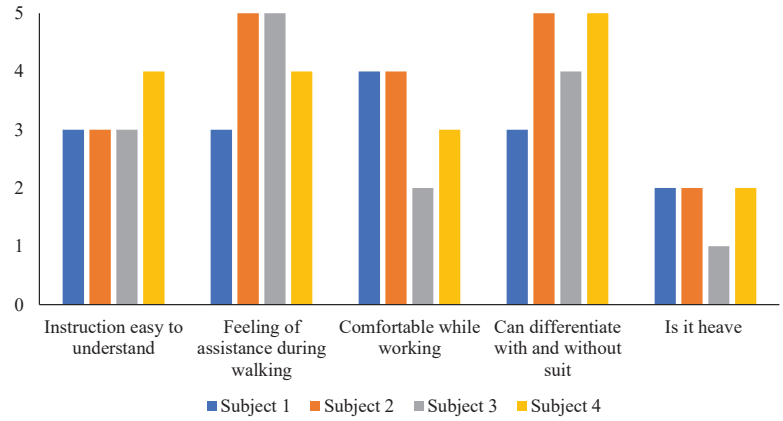

Fig. 4.6: Feedback received through questionnaire after trials of AWS.

disturbs the individual workspace or motion. The young female tested the suit for asks such as loading and unloading food packets for chicken in poultry farm, surveying the rice field and farm while walking up and down the slope. Whereas the young male tested the suit in the rice factory. During this he walked around factory, climbing up and down the stairs. He did not find difficulty in using the suit as he felt assistance during walking, and it did not interfere with his regular tasks.

The trial with elderly farmer was conducted at his rice field. The surface at this location was uneven with slopes. The elderly felt assistive force while walking on different type of surfaces doing various tasks involved in his daily farming routine. He felt less effort were required when walking with AWS as compared to without AWS on various surfaces.

From open-ended interview with each volunteer after trial all said, walking with AWS feels easy as compared to without AWS. The suit is lightweight and does not disturbs the individual workspace or motion. The young female tested the suit for asks such as loading and unloading food packets for chicken in poultry farm, surveying the rice field and farm while walking up and down the slope. Whereas the young male

tested the suit in the rice factory. During this he walked around factory, climbing up and down the stairs. He did not find difficulty in using the suit as he felt assistance during walking, and it did not interfere with his regular tasks.

The trial with elderly farmer was conducted at his rice field. The surface at this location was uneven with slopes. The elderly felt assistive force while walking on different type of surfaces doing various tasks involved in his daily farming routine. He felt less effort were required when walking with AWS as compared to without AWS on various surfaces.

From the subjective feedbacks in all the trials we observed that walking with AWS was easier compared to unassisted walking, which complements the results obtained in the evaluation experiment conducted in laboratory. Along with this, volunteers provided additional feedback, where, for young farmers just assisted walking is not enough. They face difficulties in lifting tasks e.g. pick and place of various objects. Use of machineries are not possible due to expensive tools and small workspace. On the other hand, have elderly farmers finds assistive walking useful, because his work involves lot of walking in his rice fields. But he finds the backpack for controller and air tank disturbing while driving the truck to go from one farm to another. Modifying placement of controller and air tank will allow them to keep the suit on while driving and save time when need to use next place.

4.5 Conclusion

From the subjective feedback received from the pilot trials we observed that the assisted walking was very helpful for elderly farmer while walking around agricultural field on various surfaces and doing daily routine tasks. He could identify the difference between muscle stress with and without assistive suit found it useful. For young lady and

male farmers, the walking assist force was not so significant, but they found it useful for couple of tasks which requires longer duration of walking or standing activity in agricultural lifestyle. The AWS did not intervene in the workspace while doing various daily routines during trials. All the participants suggested that having lumbar support in addition to the walking assist will be greatly useful. Moving the controller and air tank to the lower limb will make the suit more wearable.

From these feedbacks, we believe that AWS has possibility to be used as assistive device for elderly and others. To improve the usability of the device, we are currently working on improving the wearability of the device. The changes in muscle activation and lower limb kinematics on various types of surfaces are to be identified and evaluated in near future. In addition to this, it is also possible to implement autonomous control for AWS to detect and change assistance based on the user intention. One of the limitations to the device is the portable air tank which lasts for actuation, the technique needs to devised for tank to last longer than current implementation.

Chapter 5

Conclusion and Future Work

In this paper we discussed the development and evaluation of AWS to address the limitation of previously developed UPS in terms of delay in actuation and force generating capacity of PGM due to use of pump in shoe. The actuation delay was solved by using portable compressed air tanks and the actuation control i.e. actuation and deactivation of PGM was done by using pneumatic solenoid valves. The gait detection system was developed to detect gait phases and changes in the gait phase for both lower limbs. This gait detection system identifies the time of the swing phase and control algorithm actuate PGM in the swing phase.

As discussed in the introduction section, exoskeletons were developed to support walking for disabled, rehabilitation and training post stroke or accident, help walking for abled by reducing muscle fatigue or metabolic cost of walking using clever and innovative design and control schemes suitable for the respective use cases [30]. But the exoskeleton still presents various challenges such as rigid body frame which restricts normal movement if not aligned properly, increasing metabolic cost of walking, inability to function in outside environment.

As per [31] exosuits or assistive suits can be wear easily and used for longer period of time to overcome challenges of exoskeleton for augmenting abled walking. They

also mentioned, due to the nature of assistive suit the assistive force required for augmentation is also very less as compared to exoskeleton and so as the control scheme. Pneumatic artificial muscles mimics characteristics of human muscle model. Actuating PGM at the right time during walking reduces muscle fatigue or metabolic cost of walking.

Various good control algorithms such as [32–34] were developed to detect detailed gait phases and abnormal events in the gait cycle. They also indicate requirement of magnitude of assistive force to be generated to correct the abnormal events. The objective of these algorithms is to assist abnormal gait during rehabilitation training, diagnose status of patient and performance of rehabilitation treatment mainly using exoskeleton.

The gait detection system developed in this study detects stance and swing phase of the gait cycle and assists the limb in swing phase. We allow user to decide the suitable magnitude of the assistive force by regulating supplied air pressure. This control scheme keeps the device control simple and effective and the device wearable, lightweight and portable for use in outside environment for assisting normal gait.

Evaluation of AWS shows that the selected control scheme reduces muscle efforts during walking significantly or no change is observed as shown in 3.2. We also observe in the absence of actuation control and air supply AWS provides minimalistic assistive force due to elastic nature of PGM. Which overcomes the challenge of exoskeleton for assisting abled walking discussed above. Such ability of the wearable walking assist is developed in very few exoskeletons such as [13] where the assistance is discussed based on the reduction metabolic cost of walk while using unpowered exoskeleton.

Whereas for application in rehabilitation and disabled support, AWS will need complex control schemes discussed above or develop new control schemes suitable for

soft wearable assistive suits to support abnormal gait. Additionally, changes in the design of AWS will also be needed since one PGM per limb may not be enough in such cases. As per [31, 35] dynamic control of the pneumatic artificial muscles depends on the real time knowledge of air pressure, air flow and muscle configuration such as rate of change of elongation and generated force. Using this we can assistive force can be designed for dynamic requirement of human walking. Whereas this also makes system bulky and complex because of the use of sensors such as air pressure, flow, force, rigid component required for installation of these sensors and controllers in the assistive suit and batteries. In our future research we plan to address and develop suitable pneumatic control scheme for dynamic assistive force requirement taking these factors into consideration.

Bibliography

[1] L. Garçon, C. Khasnabis, L. Walker, Y. Nakatani, J. Lapitan, J. Borg, A. Ross, and A. V. Berumen, "Medical and assistive health technology: Meeting the needs of aging populations," *Gerontologist*, vol. 56, pp. S293–S302, 2016.

[2] K. Suzuki, G. Mito, H. Kawamoto, Y. Hasegawa, and Y. Sankai, "Intention-based walking support for paraplegia patients with Robot Suit HAL," *Advanced Robotics*, vol. 21, no. 12, pp. 1441–1469, 2007.

[3] S. Toyama and G. Yamamoto, "Development of wearable-agri-robot - Mechanism for agricultural work," *2009 IEEE/RSJ International Conference on Intelligent Robots and Systems, IROS 2009*, pp. 5801–5806, 2009.

[4] Y. Ikeuchi, J. Ashihara, Y. Hiki, H. Kudoh, and T. Noda, "Walking assist device with bodyweight support system," in *2009 IEEE/RSJ International Conference on Intelligent Robots and Systems, IROS 2009*, pp. 4073–4079, oct 2009.

[5] J. Pratt, B. Krupp, C. Morse, and S. Collins, "The RoboKnee: an exoskeleton for enhancing strength and endurance during walking," in *IEEE International Conference on Robotics and Automation, 2004. Proceedings. ICRA '04. 2004*, vol. 3, pp. 2430–2435 Vol.3, apr 2004.

[6] P. Malcolm, W. Derave, S. Galle, and D. De Clercq, "A Simple Exoskeleton That Assists Plantarflexion Can Reduce the Metabolic Cost of Human Walking," *PLoS ONE*, vol. 8, no. 2, 2013.

[7] B. T. Quinlivan, S. Lee, P. Malcolm, D. M. Rossi, M. Grimmer, C. Siviy, N. Karavas, D. Wagner, A. Asbeck, I. Galiana, and C. J. Walsh, "Assistance magnitude versus metabolic cost reductions for a tethered multiarticular soft exosuit," *Science Robotics*, vol. 2, no. 2, p. eaah4416, 2017.

[8] A. T. Asbeck, K. Schmidt, and C. J. Walsh, "Soft exosuit for hip assistance," *Robotics and Autonomous Systems*, vol. 73, pp. 102–110, nov 2015.

[9] K. Schmidt, J. E. Duarte, M. Grimmer, A. Sancho-Puchades, H. Wei, C. S. Easthope, and R. Riener, "The myosuit: Bi-articular anti-gravity exosuit that reduces hip extensor activity in sitting transfers," *Frontiers in Neurorobotics*, vol. 11, no. OCT, pp. 1–16, 2017.

[10] L. N. Awad, J. Bae, K. O'Donnell, S. M. De Rossi, K. Hendron, L. H. Sloot, P. Kudzia, S. Allen, K. G. Holt, T. D. Ellis, and C. J. Walsh, "A soft robotic exosuit improves walking in patients after stroke," *Science Translational Medicine*, vol. 9, no. 400, 2017.

[11] S. Sridar, P. H. Nguyen, M. Zhu, Q. P. Lam, and P. Polygerinos, "Development of a soft-inflatable exosuit for knee rehabilitation," *IEEE International Conference on Intelligent Robots and Systems*, vol. 2017-Septe, pp. 3722–3727, 2017.

[12] A. T. Asbeck, S. M. De Rossi, K. G. Holt, and C. J. Walsh, "A biologically inspired soft exosuit for walking assistance," *International Journal of Robotics Research*, vol. 34, no. 6, pp. 744–762, 2015.

[13] S. H. Collins, M. B. Wiggin, and G. S. Sawicki, "Reducing the energy cost of human walking using an unpowered exoskeleton," *Nature*, vol. 522, no. 7555, pp. 212–215, 2015.

[14] K. Ogawa, C. Thakur, T. Ikeda, T. Tsuji, and Y. Kurita, "Development of a pneumatic artificial muscle driven by low pressure and its application to the unplugged powered suit," *Advanced Robotics*, vol. 31, no. 21, pp. 1135–1143, 2017.

[15] F. Daerden and D. Lefeber, "Pneumatic artificial muscles: actuators for robotics and automation," *European Journal of Mechanical and Environmental Engineering*, vol. 47, no. 1, pp. 11–21, 2002.

[16] K. C. Wickramatunge and T. Leephakpreeda, "Empirical modeling of dynamic behaviors of pneumatic artificial muscle actuators," *ISA Transactions*, vol. 52, no. 6, pp. 825–834, 2013.

[17] J. Sarosi, I. Biro, J. Nemeth, and L. Cveticanin, "Dynamic modeling of a pneumatic muscle actuator with two-direction motion," *Mechanism and Machine Theory*, vol. 85, pp. 25–34, 2015.

[18] S. Sen and A. Bicchi, "A nonlinear elastic transmission for variable-stiffness-actuation: Objective and design," *15th National Conference on Machines and Mechanisms, NaCoMM 2011*, pp. 1–9, 2011.

[19] C. Chou and B. Hannaford, "Static and dynamic characteristics of McKibben pneumatic artificial muscles," *Robotics and Automation, 1994.*, no. 3, pp. 281–286, 1994.

[20] G. K. Klute and B. Hannaford, "Accounting for Elastic Energy Storage in McKibben Artificial Muscle Actuators," *Journal of Dynamic Systems, Measurement, and Control*, vol. 122, no. 2, p. 386, 2000.

[21] P. K. Prasad, S. Sen, S. N. Shome, and C. Har, "Impedance estimation of a pneumatic muscle as a mechanical transmission and actuation device," *2016 IEEE 1st International Conference on Control, Measurement and Instrumentation, CMI 2016*, no. Cmi, pp. 371–375, 2016.

[22] R. W. Kressig and O. Beauchet, "Guidelines for clinical applications of spatio-temporal gait analysis in older adults," *Aging Clinical and Experimental Research*, vol. 18, pp. 174–176, apr 2006.

[23] Stastics Japan, *estat*, January 22, 2019. `http://www.stat.go.jp/data/jinsui/pdf/201901.pdf`.

[24] Stastics Japan, *estat*, January 22, 2019. `http://www.stat.go.jp/english/data/shugyou/pdf/sum2017.pdf`.

[25] JISHA, *JISHA:OSH Statistics in Japan*, October 20, 2018. `https://www.jisha.or.jp/english/statistics/index.html`.

[26] S. Toyama and G. Yamamoto, "Development of wearable-agri-robot mechanism for agricultural work," in *2009 IEEE/RSJ International Conference on Intelligent Robots and Systems*, pp. 5801–5806, Oct 2009.

[27] Y. Ikeuchi, J. Ashihara, Y. Hiki, H. Kudoh, and T. Noda, "Walking assist device with bodyweight support system," in *2009 IEEE/RSJ International Conference on Intelligent Robots and Systems*, pp. 4073–4079, Oct 2009.

[28] T. Noritsugu, D. Sasaki, M. Kameda, A. Fukunaga, , and M. Takaiwa, "Wearable power assist device for standing up motion using pneumatic rubber artificial muscles," *Journal of Robotics and Mechatronics*, vol. 19, no. 6, pp. 619–628, 2007.

[29] M. P, D. W, G. S, and D. C. D, "A simple exoskeleton that assists plantarflexion can reduce the metabolic cost of human walking," *PLoS ONE*, vol. 8, no. 2, p. e56137, 2013.

[30] N. Aliman, R. Ramli, and S. M. Haris, "Design and development of lower limb exoskeletons: A survey," *Robotics and Autonomous Systems*, vol. 95, pp. 102–116, 2017.

[31] A. T. Asbeck, S. M. De Rossi, I. Galiana, Y. Ding, and C. J. Walsh, "Stronger, smarter, softer: Next-generation wearable robots," *IEEE Robotics and Automation Magazine*, vol. 21, pp. 22–33, dec 2014.

[32] S. Oh, E. Baek, S. K. Song, S. Mohammed, D. Jeon, and K. Kong, "A generalized control framework of assistive controllers and its application to lower limb exoskeletons," *Robotics and Autonomous Systems*, vol. 73, pp. 68–77, 2015.

[33] K. Kong and M. Tomizuka, "Smooth and continuous human gait phase detection based on foot pressure patterns," *Proceedings - IEEE International Conference on Robotics and Automation*, pp. 3678–3683, 2008.

[34] K. Kong, J. Bae, and M. Tomizuka, *Impedance compensation of flexible joint actuator for ideal force mode control*, vol. 17. IFAC, 2008.

[35] C. P. Chou and B. Hannaford, "Measurement and modeling of McKibben pneumatic artificial muscles," *IEEE Transactions on Robotics and Automation*, vol. 12, no. 1, pp. 90–102, 1996.

Acknowledgments

I wish to thank my advisor, Professor Yuichi Kurita, for his advice, suggestions, encouragement and patience. He has taught me in the various research fields of human augmentation, design requirement and analysis. Tasks like this are not possible without his support and encouragement. He provided and encouraged me on various platforms which helped me in my research study.

I am also grateful to committee members Professor Toshio Tsuji and Professor Toru Yamamoto for their invaluable suggestions and opinions on this dissertation.

I am very grateful to have chance for internship experience under supervision of Dr. Soumen Sen, Principle Scientist at CSIR CMERI, Durgapur, India who taught me impedance modeling techniques for soft actuators.

I must also take this opportunity to acknowledge Mr. Yusuke Kishishita, Mr. Sushil Raut and all members of the Biological Systems Engineering Laboratory at Hiroshima University for their encouragement and support.

Prof. Shinji Kaneko and Prof. Toshiaki Kondo for all the support as collaborator during onsite team project and ideas for improvement.

Finally, my deepest gratitude goes to my family for supporting me. Without them I would not have been able to complete this work.

This Ph.D. study was partially supported by Taoyaka Program, a Leading Graduate

Education Program at Hiroshima University. The support received from the program played a significant role in my research.